2024-05-01

Study Of Morphology, Structure, And Magnetic Properties Of High Entropy Alloy Systems

Matthew G. Guerrero
University of Texas at El Paso

STUDY OF MORPHOLOGY, STRUCTURE, AND MAGNETIC

PROPERTIES OF HIGH ENTROPY ALLOY SYSTEMS

MATTHEW GARRETT GUERRERO

Master's Program in Physics

APPROVED**:**

Achmed El-Gendy, Ph.D. Chair

Felicia Manchiu, Ph.D.

Hamidreza Sharifan, Ph.D.

Stephen L. Crites, Jr., PhD.
Dean of the Graduate School

Dedication

I dedicate this thesis to my family, who have stood by me all the steps of the way. To my friends, who stood me up when I felt I could not continue. To my research professor, who showed me the true meaning of dedication and what it means to be a physicist. Finally, I want to thank God, who has shown me unending love and favor on my journey. Thank you everyone!

“Physics isn’t the most important thing. Love is.”

-Richard P. Feynman

STUDY OF MORPHOLOGY, STRUCTURE, AND MAGNETIC PROPERTIES OF HIGH ENTROPY ALLOY SYSTEMS

by

MATTHEW GARRETT GUERRERO

THESIS

Presented to the Faculty of the Graduate School of

The University of Texas at El Paso

in Partial Fulfillment

of the Requirements

for the Degree of

MASTER OF SCIENCE

Department of Physics

THE UNIVERSITY OF TEXAS AT EL PASO

May 2024

Acknowledgement

I would like to express my sincere gratitude to Dr. Ahmed A. El-Gendy for his invaluable guidance, support, and encouragement throughout the course of this research. HIs expertise and insights have been instrumental in shaping this work.

I am also deeply thankful to my lab mates for their camaraderie, assistance, and collaboration. Their fellowship has enriched not only my research experience, but also my life.

I extend my appreciation to the University of Texas at El Paso's Department of Physics for providing the necessary resources and facilities for this study. Their commitment to academic excellence has been a constant source of inspiration.

Lastly, I would like to thank my family for their unwavering love, understanding, and encouragement. Their support has been my pillar of strength throughout this academic journey.

Table of Contents

List of Tables

List of Figures

Chapter 1: Introduction

Scientific investigation and technological progress in the field of materials science have been propelled by the search for new materials with previously unheard-of qualities. High Entropy Alloys (HEAs) are a fascinating class of materials that have gained significant attention in research due to their unusual combination of structural and magnetic properties that defy accepted alloy design concepts**.** These alloys mark a paradigm change in the way that metallic systems are traditionally understood.

HEAs have been around since the 1980s, theoretically speaking. However, in 1995, Jien-Wei Yeh, a scientist from Taiwan, created the first high-entropy alloys using a method he pioneered [1]. After years of development, in 2004 he and his colleagues produced the first HEA that could tolerate very high pressures and temperatures. This spurred interest in HEA research and development globally because of its promise in numerous research domains [2].

The conventional method of alloy design prior to Yeh et al.'s introduction focused on a small number of alloying elements, frequently dominated by a single main element. This strategy was based on the need for consistency and a complete comprehension of the behavior of the alloy using established phase diagrams. For decades, it had been the accepted method for creating materials with particular qualities.

Separate from Yeh's research, British physicist Brian Cantor started studying HEAs in the 1970s. However, he didn't publish his findings until 2004, just a few months after Yeh [3]. Equiatomic FeCrMnNiCo, also referred to as the "Cantor alloy," was the alloy that Cantor studied. It was among the first HEAs to exhibit a single-phase FCC (face-centered cubic crystal structure) solid solution.

This introductory chapter will cover the basic principles behind magnetic high entropy alloys, along with the main focus of this thesis, FeNiCo based HEAs with additional principal elements consisting of Ga and Mn to observe the changes in microstructure and magnetic properties between the sample HEAs. Furthermore, chemical doping by Fe, Ni, and Co solutions to the HEA samples was performed to further observe changes in samples.

1.1 Definition

The incorporation of several principle elements, usually five or more, in about equiatomic ratios results in a highly disordered atomic structure, which characterizes HEAs [4]. The conventional wisdom that had guided alloy development was challenged by this bold strategy, creating a completely new material environment.

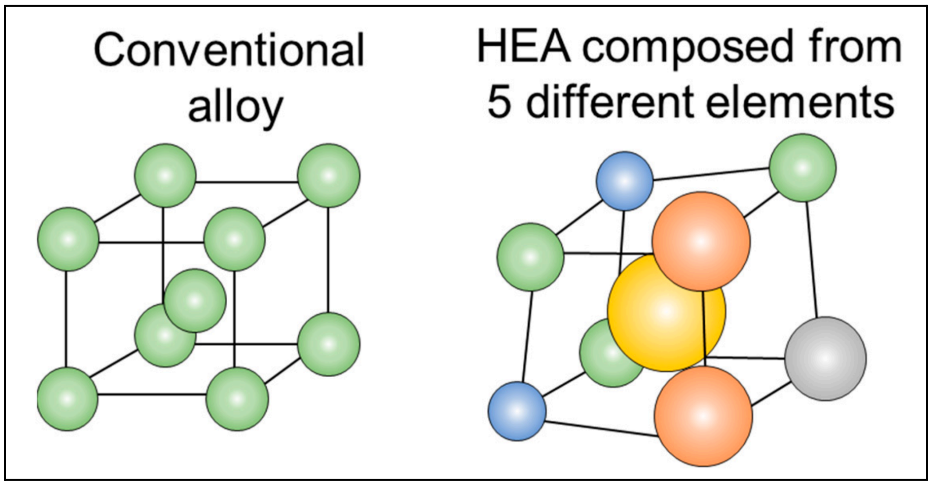

Fig 1: Illustration of an High Entropy Alloy's Structure

In spite of this, there isn't a one widely accepted description of what a HEA consists of. At least five principle elements with atomic concentrations ranging from five to thirty-five percent were needed to meet the original criteria. Additional study on the topic led to the proposition that the definition be expanded upon [5]. Because ordered phases reduce the system's

entropy, some scientists contend that only HEAs devoid of intermetallic phases may be regarded as true high entropy alloys. Some authors even assert that specific 2-4 element systems satisfy the criteria of HEAs, referring to the four major element systems as HEAs. Scientists have also proposed that alloys with a mixing entropy of between R and 1.5 R are considered "medium-entropy."

Yeh was the one who originally used the phrase "High-Entropy Alloy," attributing the solid solution phase's stabilizing factor to the high configurational energy. By contrast, Cantor was not familiar with Yeh's work and never used the term "High Entropy Alloy." He would have rather called his new materials "multicomponent alloys."

1.2 Magnetic High Entropy Alloys

Within the larger topic of high entropy alloys (HEAs), magnetic high entropy alloys (MHEAs) represent a distinct and expanding field of study [6]. MHEAs have taylored magnetic properties, which makes them attractive candidates for a variety of applications [7][8][9][10]. This is in contrast to typical HEAs, which are mostly appreciated for their mechanical and structural qualities. MHEAs differ from non-magnetic HEAs due to their magnetic ordering and behaviors, which are caused by the presence of magnetic elements like iron, cobalt, nickel, and rare-earth elements.

The ability of MHEAs to blend the advantageous aspects of magnetic materials and HEAs is what makes them significant. Researchers can customize the magnetic characteristics of MHEAs for use in magnetic refrigerators [11], actuators, and sensors [12][13] just by adjusting their microstructure**,** composition, and ratios. A wide number of industries, including electronics, telecommunications, and energy, find MHEAs appealing due to their adaptability [14][15].

1.2.1 Fe-Ni-Co Base

High entropy alloys (HEAs) that are composed of iron (Fe), nickel (Ni), and cobalt (Co) as building blocks combine mechanical and magnetic [16] in a remarkable way. These components, which are renowned for their individual ductility and strength [17], combine to form stable solid solutions in HEAs, giving the material outstanding mechanical qualities [18][19].

Fe, Ni, and Co are also ferromagnetic, which gives HEAs superior magnetic characteristics. These alloys are suited for use in magnetic devices and applications needing strong magnetic properties, such as magnetic sensors and actuators, because they can be further improved by adding additional magnetic components or applying the right heat treatment.

1.2.2 Additional Elements Mn and Ga

The properties of the high entropy alloy (HEA) FeNiCo base can be significantly altered by adding manganese (Mn) and gallium (Ga). When added to HEAs, manganese has the potential to improve mechanical qualities because it is known to boost the strength and ductility of steels, leading to solid solution phases that may result in the development of new phases.

Additionally, the soft, easily flexible metal gallium can improve the formability and machinability of the alloy [20]. Due to its larger size, gallium can occupy lattice interstitial spaces, which might change the electronic structure of the alloy [21][22].

Combining together the manganese and gallium with the FeNiCo base in a HEA can produce a complex microstructure that may include novel intermetallic phases as well as solid solution phases. Improved strength, ductility, machinability, or magnetic properties, for instance, could result from the combination of gallium and manganese, opening up new uses for the alloy.

1.3 Magnetism

The history of magnetism goes back thousands of years, when certain naturally occurring magnetic elements, such as lodestone, were recognized by early civilizations for their special qualities. These characteristics, like magnets' capacity to attract iron, were initially recorded by the ancient Greeks and Chinese. But it wasn't until the 19th century that researchers started using theoretical models and experiments to gain a more methodical grasp of magnetism. Ferromagnetism, antiferromagnetism, paramagnetism, and superparamagnetism are the four forms of magnetism that are frequently seen in MHEAs.

1.3.1 Ferromagnetism

Ferromagnetism is the state in which the magnetic moments of individual atoms align in the same direction to produce a high overall magnetic field. This phenomenon is seen in some materials, such as iron, nickel, cobalt, and several rare-earth metals. For ferromagnetic materials, this alignment happens naturally below a temperature known as the Curie temperature (T_c).

Neighboring atoms' magnetic moments interact at temperatures below T_c, leading them to align parallel to one another in an effort to minimize energy. All of the atomic magnetic moments within the material align to produce magnetic domains as a result of this alignment. Every domain functions as a little magnet would, having a north and south pole; but, on a wider scale, these domains' magnetic moments are randomly orientated, leaving no net magnetic field.

The domains of a ferromagnetic material begin to align with an external magnetic field when it is applied. A large magnetic moment for the material as a whole can be produced if the external field is strong enough to cause the bulk of the domains to align in that direction. The domains may interact to keep the alignment after the external field is withdrawn, leaving the material with residual magnetization.

Hysteresis, or the delay between the application and removal of an external magnetic field and the material's response, is one of the essential characteristics of ferromagnetic materials. Ferromagnetic materials are advantageous for permanent magnets and magnetic storage devices because of their hysteresis behavior, which enables them to maintain their magnetization even in the absence of an external field.

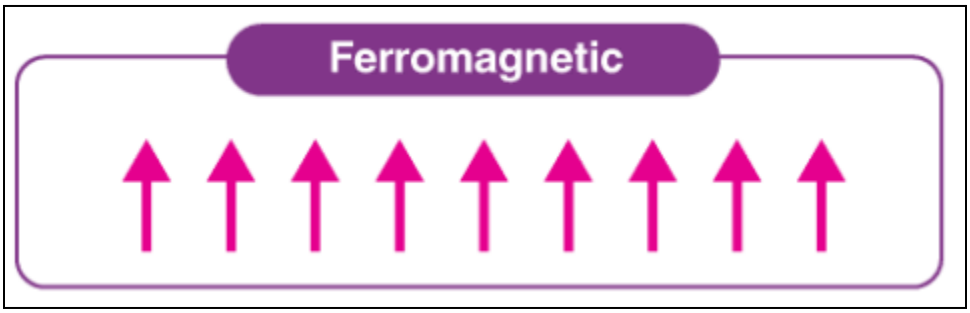

Fig 2: Ferromagnetic domains after exposure to external magnetic field

1.3.2 Antiferromagnetism

When nearby magnetic moments line up in opposing directions, a material's net magnetic moment becomes zero, a phenomenon known as antiferromagnetism. This is in direct contrast to ferromagnetism, which exhibits the characteristic in which magnetic moments are aligned parallel to one another.

Because of competing interactions, the magnetic moments of nearby atoms or ions tend to align antiparallel to one another. By minimizing the material's total magnetic energy, this alignment creates magnetic domains where neighboring spins cancel each other out. Therefore, in the absence of an applied external magnetic field, antiferromagnetic materials do not display a macroscopic magnetic moment.

These domains can be reoriented to align with an applied external magnetic field, giving rise to a net magnetic moment for the material. On the other hand, the material reverts to its antiferromagnetic condition when the external field is removed.

A material exhibiting antiferromagnetism has a Néel temperature (T_N) above which thermal energy causes the antiparallel alignment of magnetic moments to be disrupted, turning the material paramagnetic. The material displays antiferromagnetic order below T_N, with atoms or ions arranged in alternating layers or sublattices that have opposite magnetic moments.

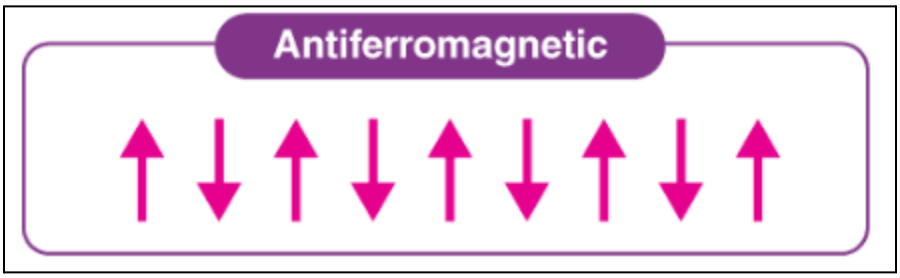

Fig 3: Antiferromagnetic orientation following exposure to an external magnetic field

1.3.3 Paramagnetism

In the absence of an external magnetic field, paramagnetism is a type of magnetism that is seen in materials where the magnetic moments of individual atoms or ions are randomly orientated. Paramagnetic materials do not have a net magnetic moment because the random orientations cancel each other out.

A weak magnetization is produced when a paramagnetic material is exposed to an external magnetic field because the atoms' or ions' magnetic moments prefer to line up with the field. However, as the external field is eliminated, this alignment vanishes. A paramagnetic material's degree of magnetization is directly correlated with its susceptibility—a measure of how readily it can get magnetized—and the strength of the applied magnetic field.

When a material's atoms or ions have unpaired electrons, paramagnetism is the result. The observed magnetic behavior can be caused by these unpaired electrons' magnetic moments aligning with an external magnetic field. Positive magnetic susceptibility, or the ability to be drawn to magnetic fields, is a characteristic of paramagnetic materials.

Curie's law, which explains the relationship between magnetism and temperature in paramagnetic materials, is one of the essential characteristics of paramagnetic materials. A paramagnetic material's magnetization is inversely proportional to temperature, which means that as the temperature rises, the material's magnetism decreases. In comparison to ferromagnetism and antiferromagnetism, paramagnetism is a weaker type of magnetism.

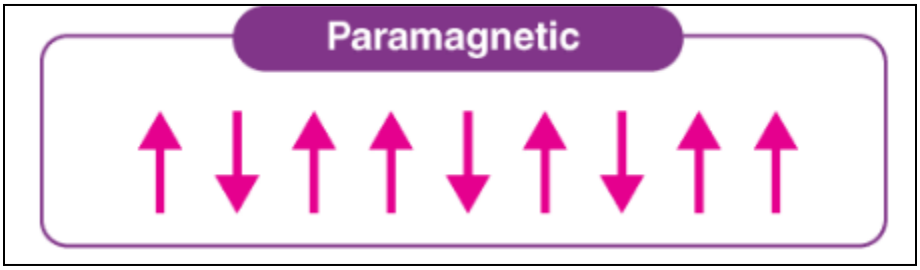

Fig 4: Orientation of paramagnetic after being exposed to an external magnetic field

1.3.4 Superparamagnetic

The magnetic moments of nanoparticles or nanoclusters can oscillate between two or more stable states in the absence of an external magnetic field, a phenomenon known as superparamagnetism that has been seen in some materials, notably several high entropy alloys (HEAs). This effect results from the nanoparticles' finite size, which lets temperature fluctuations affect their magnetic moments.

When an alloy has magnetic phase nanoparticles or nanoclusters below a threshold size known as the superparamagnetic limit, superparamagnetism can arise. Below this threshold, the magnetic anisotropy energy can be overcome by thermal fluctuations, leading to the random orientation flipping of the magnetic moments of the nanoparticles.

However, because superparamagnetism in HEAs depends on the size, makeup, and distribution of the magnetic nanoparticles, it can be difficult to manage and exploit. Through

careful alloy design and processing methods, researchers are currently investigating ways to modify the magnetic properties of HEAs, including the occurrence of superparamagnetism.

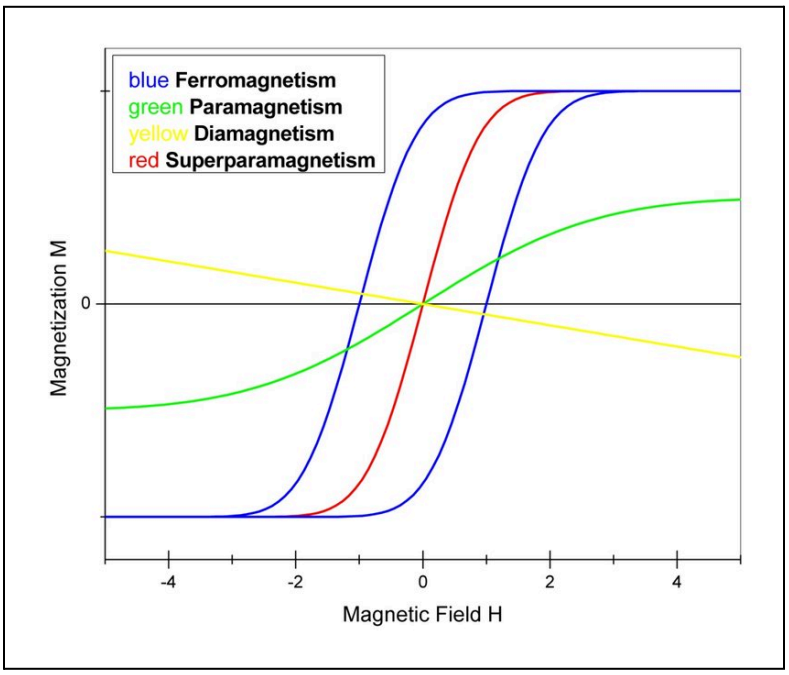

Fig 5: Hysteresis loop with magnetism types

Chapter 2: Synthesis

Numerous methods are available for the synthesis of high entropy alloys (HEAs), each with specific benefits and drawbacks. The traditional method of arc melting is melting elemental or pre-alloyed powders or bulk material of high purity in a regulated environment and rapidly solidifying the resulting alloy. Although this approach is straightforward and efficient, it may result in non-uniform microstructure and composition. Another popular method is ball milling, which uses high energy to grind constituent powders into solid-state alloys. Long milling times are necessary for this approach, but it delivers good compositional homogeneity. These two approaches are applied in this research, along with chemical doping.

Additional synthesis methods for high-energy alloys (HEAs) include powder metallurgy (PM) processes like hot pressing and spark plasma sintering, which provide fine-grained control over microstructure and composition. HEAs with intricate geometries can also be created by additive manufacturing, or 3D printing. High-pressure torsion and other severe plastic deformation (SPD) techniques can yield ultrafine-grained HEAs with improved characteristics.

For the manufacture of HEAs, hybrid approaches that combine two or more synthesis procedures have also been established. For instance, completely dense HEAs with customized microstructures have been created by combining ball milling and spark plasma sintering. These approaches minimize the drawbacks of each methodology while combining the benefits of several.

2.1 Arc Melting

One popular technique for producing high entropy alloys (HEAs) is arc melting. It entails creating a high-energy electric arc between a tungsten electrode and the HEA precursor materials to melt a combination of bulk or pre-alloyed powders of high purity. Usually, this procedure is

conducted in a regulated environment, such as vacuum or argon, to avoid oxidation and guarantee the purity of the final alloy.

Since arc melting can quickly melt and solidify the alloy, producing a homogeneous microstructure, it is especially well-suited for HEA synthesis. The production of a totally molten alloy is made possible by the high temperatures reached during arc melting, which guarantees complete mixing of the constituent elements. When compared to alternative synthesis techniques, this results in a microstructure and composition that are more consistently homogenous.

Arc melting equipment is very basic and can easily be scaled up for commercial output. Furthermore, arc melting is a flexible technique for producing HEAs with a variety of properties since it can handle a broad range of alloy compositions.

Arc melting does, however, have some restrictions. The high temperatures involved may cause volatile components to evaporate and be lost, changing the alloy's ultimate composition. Arc melting also necessitates meticulous control of process variables like arc voltage and current in order to guarantee the appropriate microstructure and composition of the HEA.

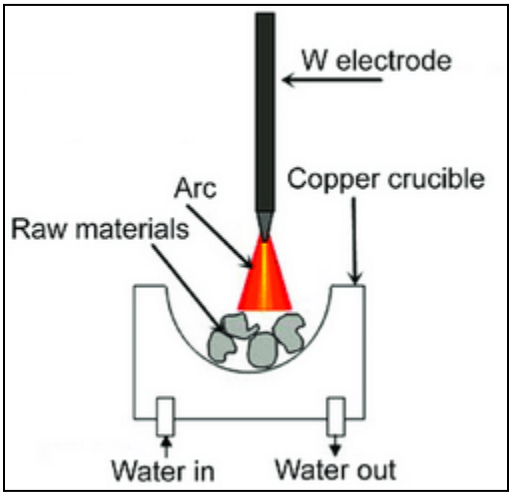

Fig 6: Representation of the function of Arc Melting

2.2 Ball Milling

The synthesis of high entropy alloys (HEAs) can be achieved by the widely utilized ball milling method, which can be easily scaled up for industrial production as well and achieves high levels of compositional homogeneity. High-energy mills are used in ball milling to mechanically alloy powdered elements.

The potential of ball milling to produce compositional homogeneity in HEAs is one of its main benefits. The equal distribution of elements throughout the alloy is achieved by facilitating the mixing of elemental powders at the atomic level through the high-energy impacts produced during milling. This is especially crucial for HEAs, whose special qualities depend on the presence of several elements in almost equimolar ratios.

The adaptability of ball milling in alloy design is an additional benefit. Elements that are challenging to combine with traditional techniques, including elemental powders with wildly disparate melting temperatures or reactivity, can be alloyed via ball milling. Furthermore, doping materials can be added to the alloy during the ball milling process to modify its characteristics, such as increasing its magnetic or mechanical strength.

Ball milling does ha**ve** certain drawbacks in addition to its benefits. The use of high-energy ball mills can lead to contamination from the milling medium, and the operation can be time-consuming, especially when trying to achieve tiny microstructures. Nevertheless, by carefully regulating the milling parameters and using the proper milling media, these limits can be lessened.

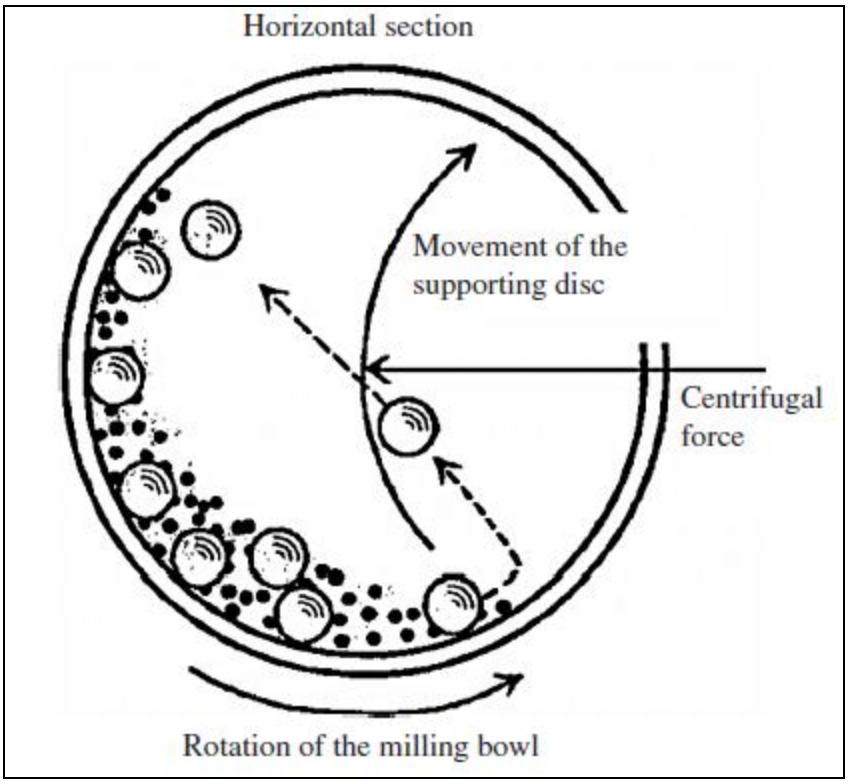

Fig 7: Representation of the process of Ball Milling

2.3 Chemical Doping

Chemical doping is the deliberate process of adding impurities or dopants into a substance in order to alter its properties. Chemical doping is a technique that can be used to increase the concentration of specific elements in high entropy alloys (HEAs), changing the alloy's mechanical properties, microstructure, and other attributes.

Adding trace amounts of a dopant element to the alloy during the manufacturing process is a popular technique for chemical doping in high-energy alloys. Usually, the dopant element is selected based on its capacity to modify the alloy's properties in a way that is desirable. For instance, doping HEAs with elements like boron, carbon, or nitrogen can increase their hardness and strength by producing solid solutions or secondary phases that prevent dislocation migration.

Reactive milling methods, like mechanical alloying, are another way to introduce dopant elements into the alloy for chemical doping in HEAs. High-energy ball milling of elemental powders is the process of mechanical alloying, which produces solid-state alloys. Dopant elements can be precisely controlled during the milling process by adding them to the milling media or introducing them as gas to alloy with the powder particles.

2.4 High Entropy Alloy Synthesis

2.4.1 Arc Melter Synthesis

The synthesis of the base FeNiCo was done in order to compare the results of the succeeding HEA compositions with each other. Equiatomic ratios for Fe, Ni, and Co were used to separate the 99.9% pure metals, each weighing roughly 1g, from their bulk material. Prior to adding bulk material, the appropriate ratios for Mn or Ga were also cut off for HEA samples that required them. After making sure there were no leftover impurities from earlier tests, the materials were put into a copper crucible that had been thoroughly cleaned using a solution of pure ethanol and coarse sandpaper. Because of its reactivity, manganese was usually deposited at the bottom, followed by gallium when applicable, then iron, nickel, and cobalt in any order.

After that, the crucible was sealed and put into the arc melter apparatus. A vacuum is created by pumping all of the air out of the chamber. To establish an argon-enriched atmosphere for the synthesis of HEA, argon was then pumped in. This is because argon minimizes oxidation due to its inert nature. The arc melter was made operational by turning on a high voltage power supply. The next step would be to melt each HEA sample several times, being sure to turn the sample over in between melts to encourage uniform dispersion of the elements. After the sample

had been synthesized into a fresh HEA, it would be taken out of the chamber and stored safely in a glass container.

2.4.2 Ball Milling

After that, the containers containing the HEA samples, FeNiCo, $FeNiCoMn_{0.2, 0.4, 0.6}$, $FeNiCoMn_{0.2}Ga_{0.1, 0.3}$, and $FeNiCoGa_{0.2}$ were removed and sliced in half. One of the halves would then be methodically chopped into pieces that became progressively smaller until they averaged around 1 cm, and the unused half would be returned to its container. After flattening the chunks in a metal mortar and pestle, the pieces would be cut again into smaller bits, this time to a size of around 3 mm.

After that, hexane was added to a ball miller canister containing these tiny fragments. Hexane, an oxygen-free organic solvent, is employed as a lubricant and to stop any oxidation during the grinding process. After that, this is put inside the ball mill. Every HEA would be milled for two, four, and six hours, with a sample being obtained for additional testing at each interval. Any remaining nanomaterials that were still adhered to the surfaces would thereafter be removed from the canister.

2.4.3 Chemical Doping

Following a six-hour ball milling process, the HEA samples from $FeNiCoMn_{0.2}$ and $FeNiCoMn_{0.2}Ga_{0.1}$ were collected and chemically doped. Excess iron would be added to the HEA sample during the reaction procedure by introducing the samples to the $FeSO_4$ and $NaBH_4$ reaction. This excess dopant could potentially alter the HEA's magnetic and structural properties, resulting in distinct characteristics to be seen, and thus were manufactured. Excess Co and excess Ni were separately added to the same initial six hour ball milled $FeNiCoMn_{0.2}$ and $FeNiCoMn_{0.2}Ga_{0.1}$ HEAs in identical experiments.

Chapter 3: Experimental Procedures

3.1 Vibrating Sample Magnetometer

A Vibrating Sample Magnetometer (VSM) is a device for measuring the magnetic characteristics of materials. It is an extremely sensitive device that can determine how a sample's magnetization changes with the strength and direction of a magnetic field. VSMs are widely used to research the magnetic behavior of many materials, in this case high entropy alloys (HEAs), in materials science, physics, and engineering.

The magnetization of a sample as a function of applied magnetic field is the primary measurement made by a VSM. The magnetic properties of the material, including its coercivity, magnetic susceptibility, and magnetic moment, are revealed by this measurement. An extremely sensitive detector is used to measure the magnetization that results from applying a magnetic field to the sample in order for the VSM to function.

Coercivity is a measurement of a substance's resistance to demagnetization, while remanence is the magnetism that remains in a material after the applied magnetic field is removed. These measurements offer important insights on a material's stability and magnetic behavior.

Utilizing a vibrating sample magnetometer (VSM) VersaLab 3 Tesla (VSM) from Quantum Design, the magnetic characteristics of the HEA were examined. At 300 K, and between 50 and 400 K, the hysteresis loop, or MxH, was measured.

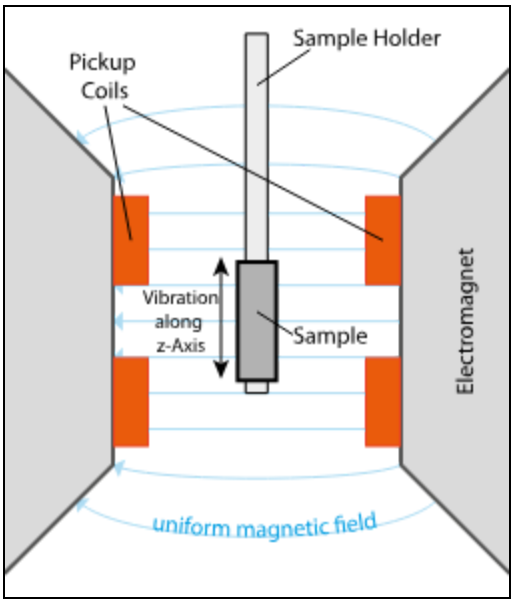

Fig 8: Illustration of VSM and the way in which data is gathered

3.2 Scanning Electron Microscopy

A Scanning Electron Microscope (SEM) is a potent instrument for high-resolution surface imaging and analysis. In order to produce comprehensive images and obtain data regarding the composition and structure of the sample, it operates by directing a concentrated electron beam across the sample's surface and detecting different signals, including secondary electrons, backscattered electrons, and X-rays.

SEM is frequently used to examine the microstructure, morphology, and elemental distribution of high entropy alloys (HEAs). SEM's high-resolution pictures can provide information about an alloy's flaws, phase composition, and grain structure. Understanding these details is essential to comprehending the characteristics and actions of HEAs.

This thesis uses energy-dispersive X-ray spectroscopy (EDS), although wavelength-dispersive X-ray spectroscopy (WDS) can also be employed with SEM to undertake elemental analysis of HEAs. Using these methods, scientists may map the distribution of

elements in the sample and ascertain the alloy's elemental composition. This data is crucial for describing the composition of the alloy and locating any elemental segregation or grouping.

Additionally, electron backscatter diffraction (EBSD) and other methods can be utilized with SEM to investigate the mechanical characteristics of HEAs. By mapping the crystallographic orientation of the alloy's grains, researchers can use EBSD to get insight into the mechanical behavior of the material, including its deformation mechanisms and grain boundary properties.

Using a Hitachi S-4800 Field Emission Scanning Electron Microscope (FE-SEM), the measurements were made in order to characterize the morphology, particle size, and elemental mapping of the HEA samples.

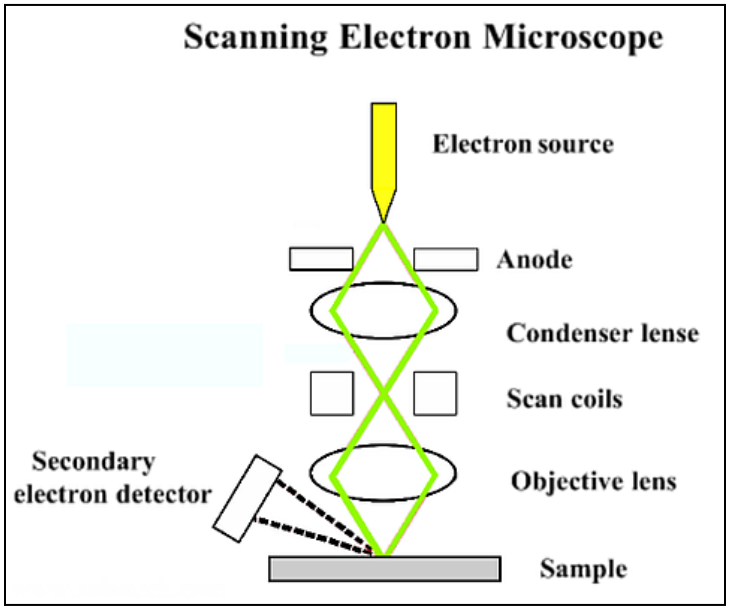

Fig 9: Illustration of SEM and the way in which data is gathered

3.3 X-ray Diffraction

The method of X-ray diffraction (XRD) is used to examine a material's crystal structure. It operates by pointing an X-ray beam onto a sample, which causes the beam to scatter in a way that is determined by the material's atomic arrangement. Researchers can ascertain the crystal

structure, phase composition, and other structural characteristics of the material by calculating the angles and intensities of the scattered X-rays.

X-ray diffraction (XRD) is a widely utilized analytical tool in the investigation of crystallographic phases and structural features of high entropy alloys (HEAs). HEAs are renowned for having intricate crystal structures that can contain several phases as well as solid solutions. These phases can be recognized and their relative amounts in the alloy can be ascertained with the aid of XRD.

The diffraction pattern formed by the dispersed X-rays is one of the important measurements obtained by XRD for HEAs. The atomic planes in the material's crystal structure are represented by the peaks in this pattern. The locations and intensities of these peaks reveal details about the alloy's grain size, lattice characteristics, and crystal structure. Using Cu Kα radiation (k = 0.1548 nm), the PANalytical X'Pert PRO XRD diffractometer produced the crystal structure characterisation of the HEA nanoparticles.

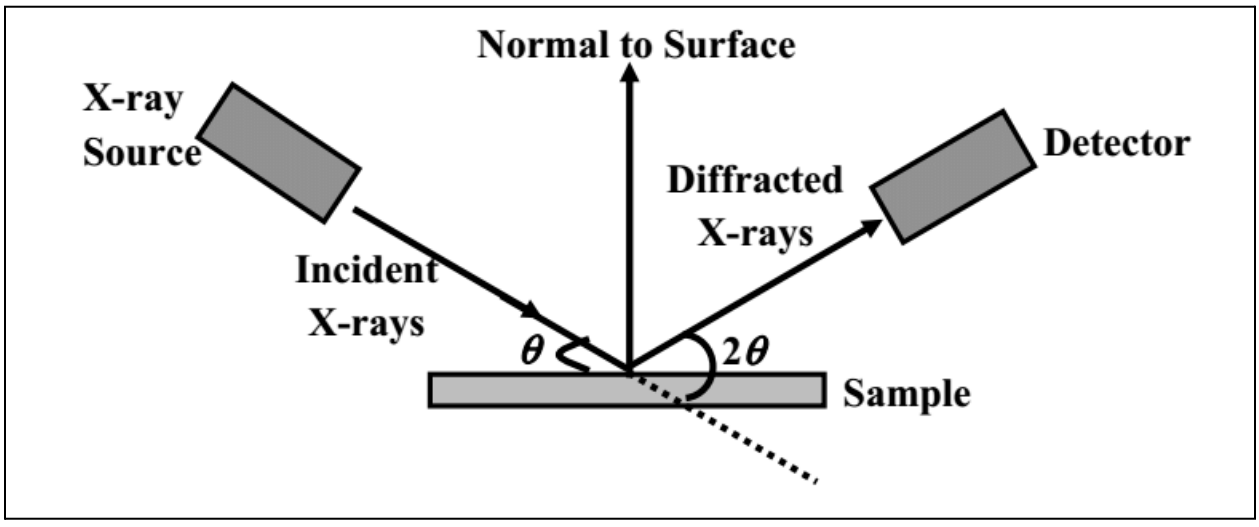

Fig 10: Illustration of SEM and the way in which data is gathered

Chapter 4: Characterization

4.1 Magnetic Properties Without Chemical Doping

Investigations on the magnetic characteristics of the magnetic HEA samples have been conducted at 3T and 300K magnetic fields and temperatures. Remarkably, all of the HEA samples, FeNiCo, $FeNiCoMn_{0.2,\ 0.4,\ 0.6}$, $FeNiCoMn_{0.2}Ga_{0.1,\ 0.3}$, and $FeNiCoGa_{0.2}$ exhibit superparamagnetic behavior. This is indicated by their closed hysteresis loops.

The data indicates that the base FeNiCo alloy demonstrates the greatest paramagnetic behavior, which was to be expected. The inclusion of manganese lowers the magnetics saturation in exchange for better mechanical properties. The more manganese added, the greater the loss of magnetic properties. For this reason $Mn_{0.2}$ was chosen as the ratio for the gallium HEA samples, low enough to have minimal impact on magnetic saturation, but great enough to still impact the morphology and structure of the HEA.

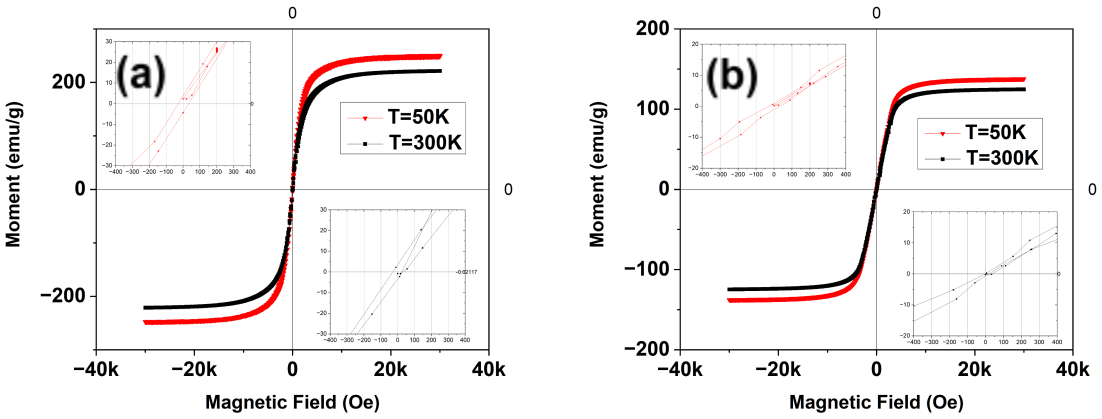

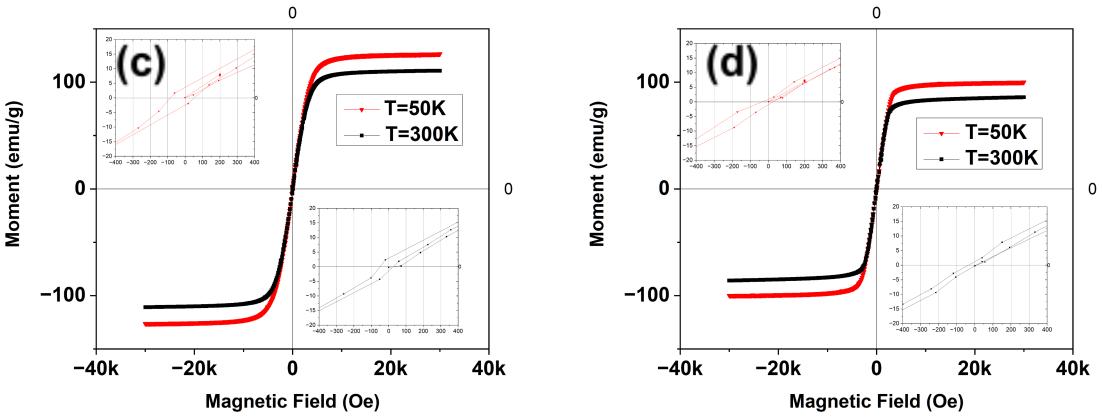

Fig. 11: Magnetic hysteresis loops of HEAs (a) FeNiCo, (b) FeCoNi($Mn_{0.2}$), (c) FeNiCo($Mn_{0.4}$), (d) FeNiCo($Mn_{0.6}$) with inset representing magnified view of central region

Gallium was chosen due to its soft metallic behavior and its potential to improve the electrical properties of the manganese HEA sample. To compare the findings of the previous experiments, a sample was created, $FeNiCoGa_{0.2}$, to examine whether manganese and gallium together could produce a unique morphology and structure. Low gallium ratios were chosen to prevent further loss of magnetic ability of the sample, and to preserve mechanical stability due to the increasing presence of gallium's unique mechanical properties affecting the sample's structure.

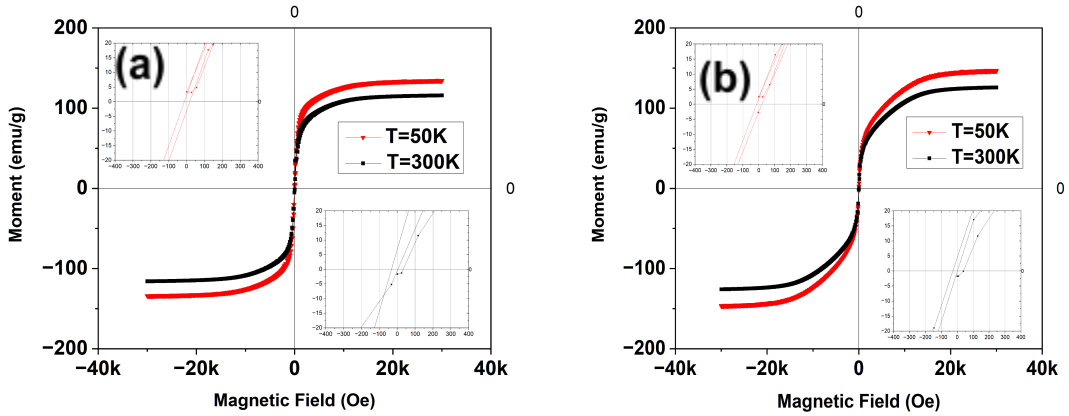

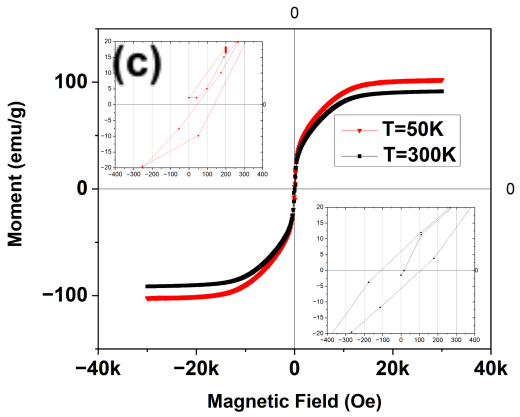

Fig. 12: Magnetic hysteresis loops of HEAs of (a) FeNiCo($Mn_{0.2}Ga_{0.1}$), (b) FeNiCo($Ga_{0.2}$), (c) FeNiCo($Mn_{0.2}Ga_{0.3}$) with inset representing magnified view of central region

From all the data, and shown in Table 1, the FeNiCo base alloy demonstrated the highest magnetic saturation and plateau. The $FeNiCoMn_{0.2}$ and the $FeNiCoGa_{0.2}$ were 3rd and 2nd highest in magnetic saturation respectively. However, the $FeNiCoMn_{0.2}Ga_{0.1}$ sample placed 4th overall.

Sample	Peak Magnetic Saturation at 50K (emu/g)	Peak Magnetic Saturation at 300K (emu/g)
FeNiCo	250.358	221.438
FeNiCo($Mn_{0.2}$)	137.803	124.752
FeNiCo($Mn_{0.4}$)	126.57022	110.869
FeNiCo($Mn_{0.6}$)	99.981	85.93644
FeNiCo($Mn_{0.2}Ga_{0.1}$)	134.391	115.928
FeNiCo($Ga_{0.2}$)	147.018	125.871
FeNiCo($Mn_{0.2}Ga_{0.3}$)	102.376	91.430

.

Table 1: Magnetic Saturation Peaks of the various HEA samples at both 50K and 300K

4.2 Structure and Morphology Without Chemical Doping

4.2.1 XRD Analysis

4.2.1.1 Manganese HEA Samples

The arrangement of atoms within a material, along with the kinds and amounts of elements present, have a significant impact on the position and intensity of peaks in an XRD graph. The following figures display the results of the XRD study performed on the FeNiCo, FeNiCo, FeNiCo($Mn_{0.2}$), FeNiCo($Mn_{0.4}$), and FeNiCo($Mn_{0.6}$). The graphs display similar FCC (face-centered cubic) FeNi hkl peaks, indicating that the FeNiCo($Mn_{0.2, 0.4, 0.6}$) HEA likewise has a simmilar FCC crystal structure. It also demonstrates that the inclusion of manganese has affected the lattice characteristics and led to some shifts in the peak positions and intensities resulting in the distinct XRD pattern from the FeNi FCC.

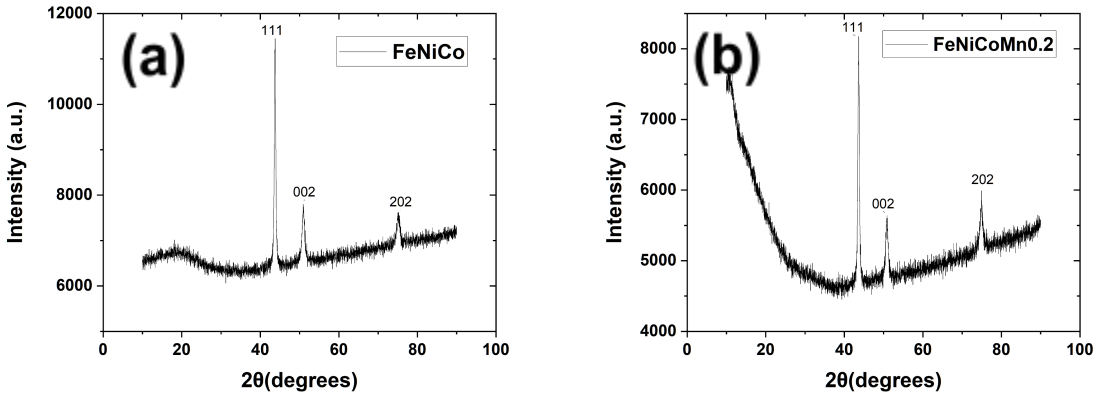

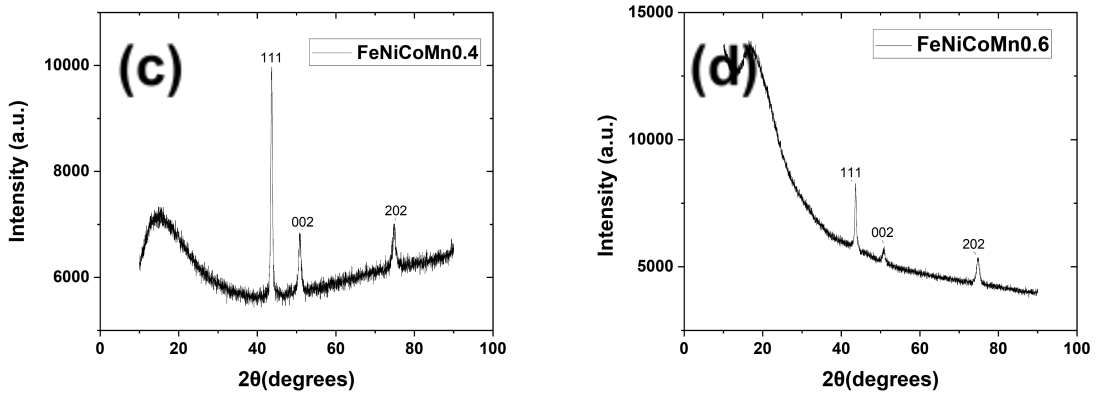

Fig. 13 XRD patterns of (a) FeNiCo, (b) FeNiCo($Mn_{0.2}$), (c) FeNiCo($Mn_{0.4}$), and (d) FeNiCo($Mn_{0.6}$)

4.2.1.2 Gallium HEA Samples

Similar principle elements should predict the presence of similar peak types in the gallium samples. Gallium, however, had a comparable effect in the following circumstances, where its addition was connected with changes in the intensity of the FeNiCo graph peaks. This implies that the gallium affected the lattice parameters and caused the changes observed, but not significantly enough to make the samples distinct from the previous manganese samples. The alteration manganese has already introduced had a much greater impact than the gallium, however.

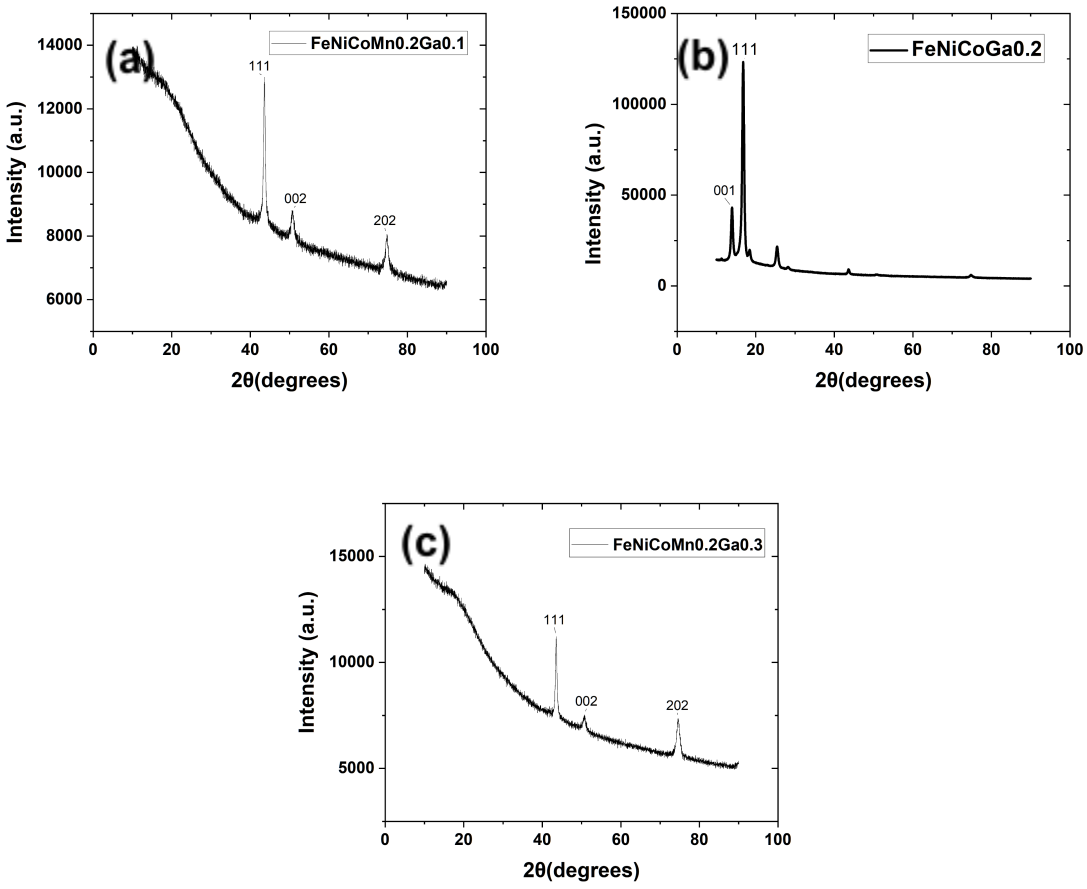

Fig. 14 XRD patterns of (a) FeNiCo($Mn_{0.2}Ga_{0.1}$), (b) FeNiCo($Mn_{0.2}Ga_{0.3}$), and (c) FeNiCo($Ga_{0.2}$)

4.2.2 EDS Analysis

4.2.2.1 Manganese HEA Samples

Iron (Fe), nickel (Ni), cobalt (Co), and manganese (Mn) were the principal elements represented by peaks on the EDS graphs for the FeNiCo, FeNiCo($Mn_{0.2}$), FeNiCo($Mn_{0.4}$), and FeNiCo($Mn_{0.6}$) HEAs. Trace elements from the material employed to keep the sample in place were also visible. Furthermore, the EDS plots for the HEAs containing Mn also had peaks that corresponded to Mn. These findings imply that Mn was successfully incorporated into the HEA samples , helping to explain the observed changes in phase composition and particle size.

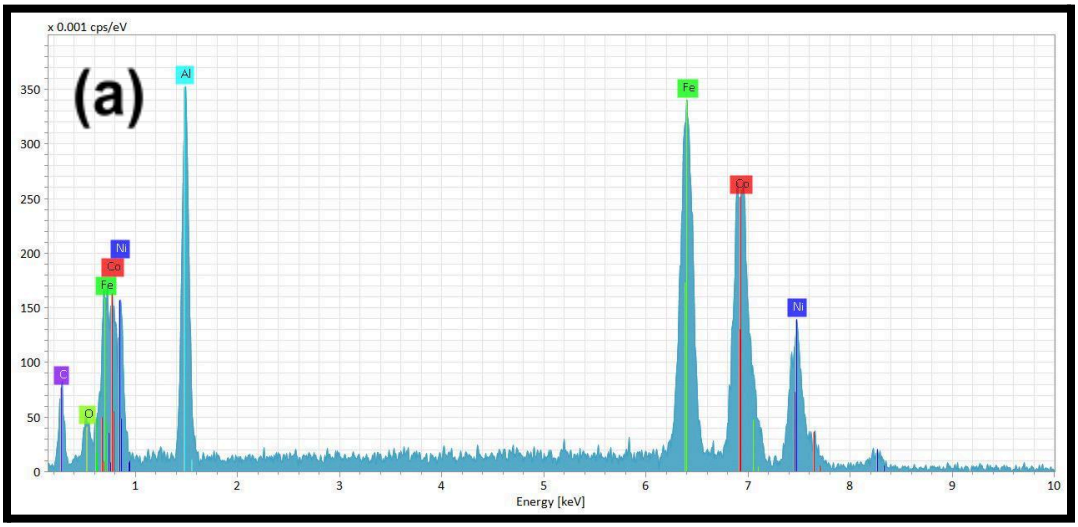

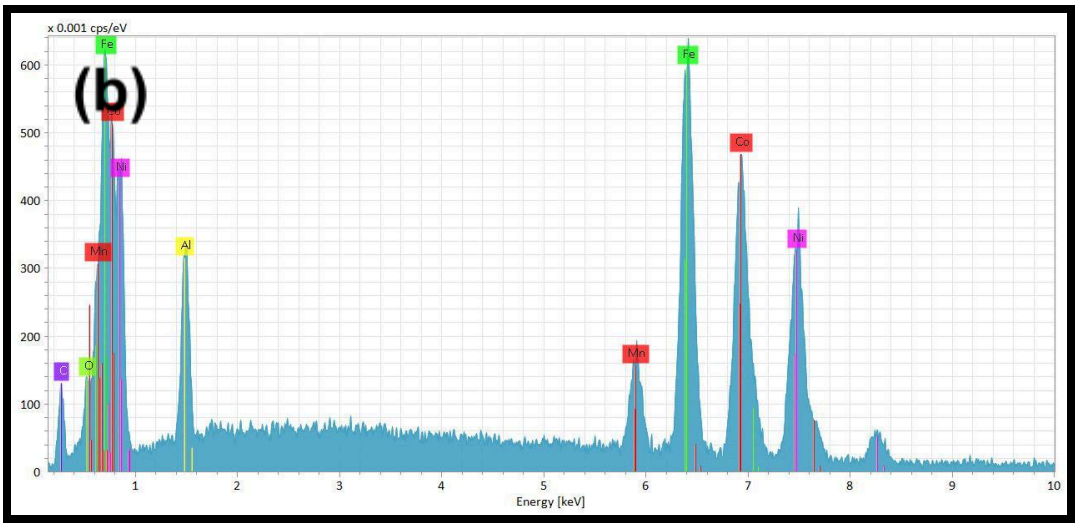
x 0.001 cps/eV
(b)
Fe
Co
Ni
Mn
Al
C
O
Energy [keV]

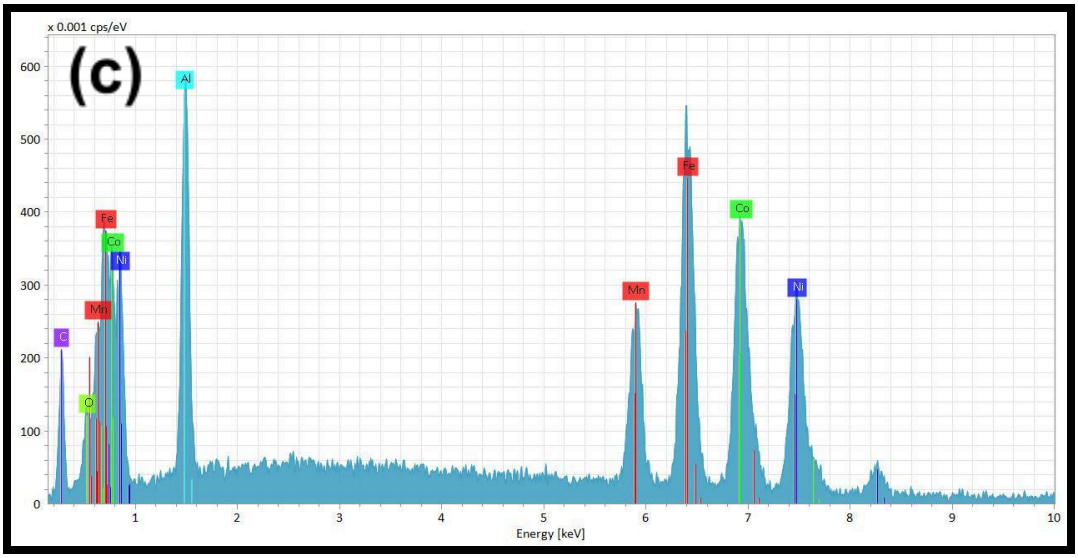
x 0.001 cps/eV
(c)
Al
Fe
Co
Ni
Mn
C
O
Energy [keV]

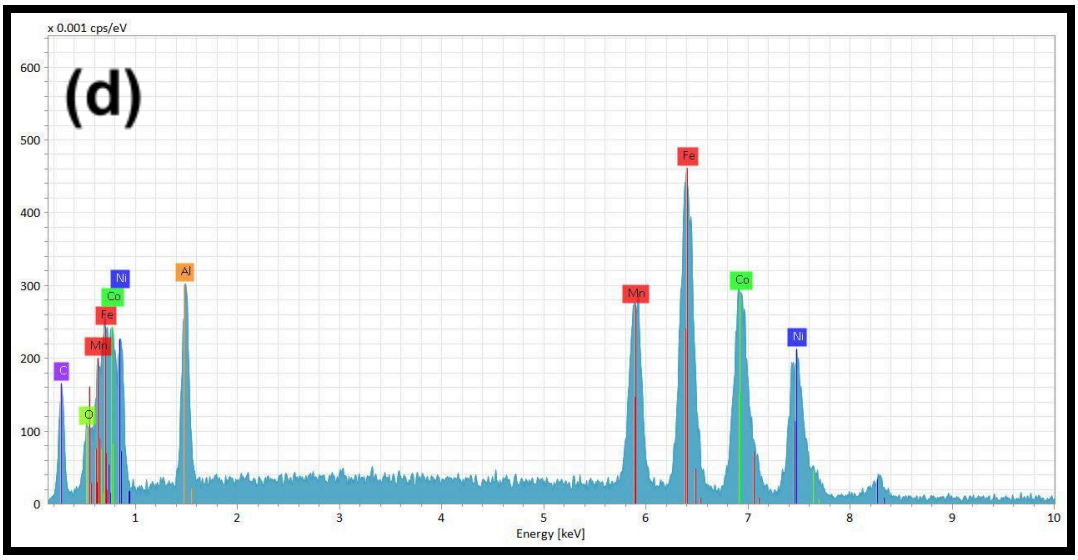

Fig. 15 EDS patterns of (a) FeNiCo, (b) FeNiCo($Mn_{0.2}$), (c) FeNiCo($Mn_{0.4}$), and (d) FeNiCo($Mn_{0.6}$)

4.2.2.2 Gallium HEA Samples

Iron (Fe), nickel (Ni), cobalt (Co), manganese (Mn), and gallium (Ga) were represented by peaks on the EDS graphs corresponding to the FeNiCo($Mn_{0.2}Ga_{0.1}$), FeNiCo($Ga_{0.2}$), and FeNiCo($Mn_{0.2}Ga_{0.3}$) HEAs. Trace elements were also present**.** These peaks were caused by the material used to hold the sample in place. The data implie**s** that gallium was also successfully added to the HEAs along with the manganese leading to a change in the observed morphology. One thing to note however, is the uneven levels of Fe, Ni, and Co present in the samples. This is typical of HEA designs with non equiatomic ratios. Further synthesis methods could be utilized to minimize this.

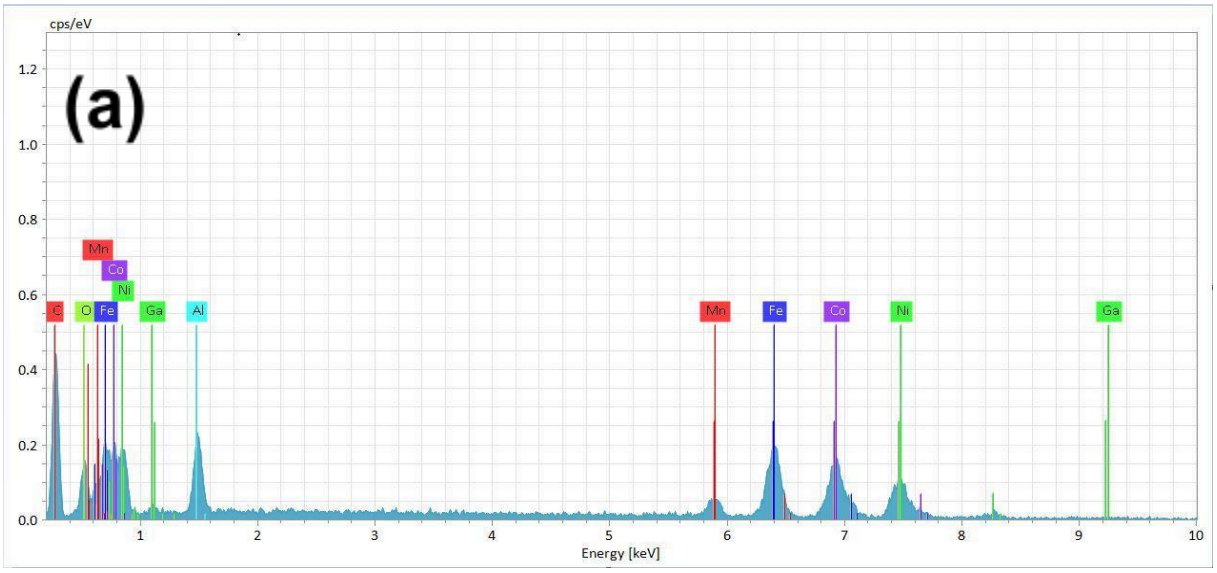
cps/eV
(a)
Mn
Co
Ni
C
O
Fe
Ga
Al
Mn
Fe
Co
Ni
Ga
Energy [keV]

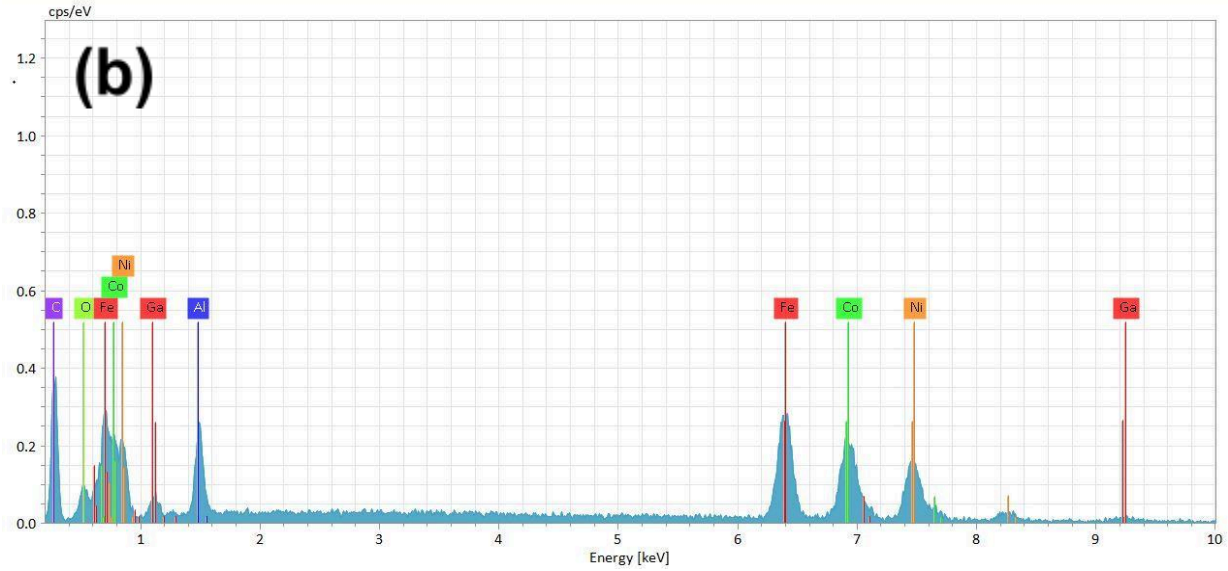
cps/eV
(b)
Ni
Co
C
O
Fe
Ga
Al
Fe
Co
Ni
Ga
Energy [keV]

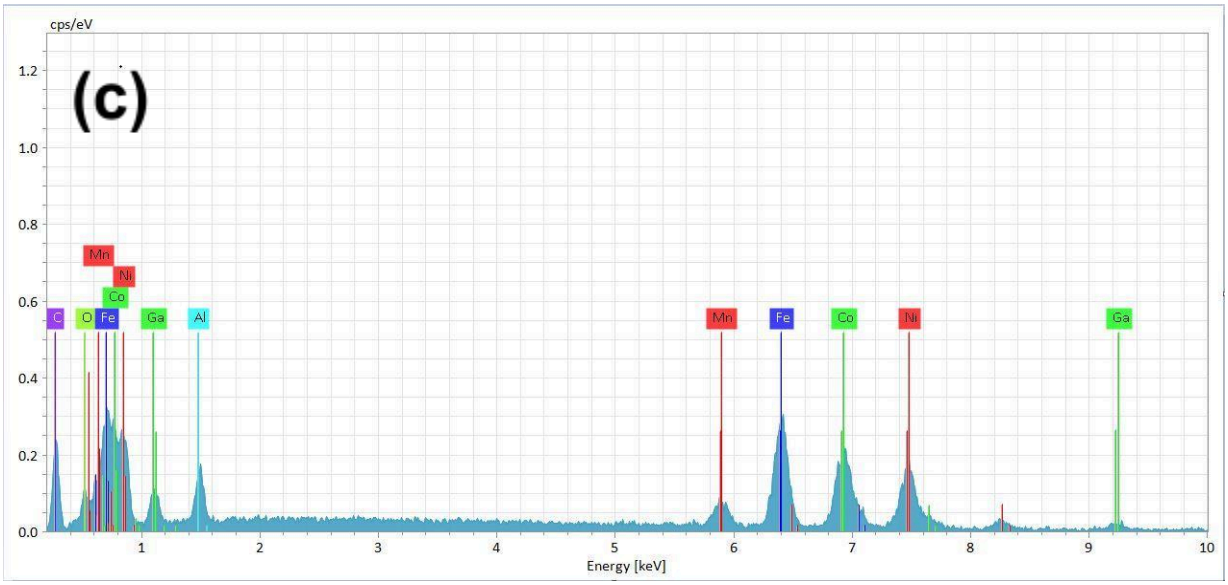

Fig. 16 EDS patterns of (a) FeNiCo($Mn_{0.2}Ga_{0.1}$), (b) FeNiCo($Ga_{0.2}$), and (c)FeNiCo($Mn_{0.2}Ga_{0.3}$)

4.2.3 SEM Analysis

Grain sizes in the samples vary widely, according to data obtained from SEM imaging of FeNiCo, FeNiCo($Mn_{0.2}$), FeNiCo($Mn_{0.4}$), and FeNiCo($Mn_{0.6}$). The largest grains that were seen were flakes that measured about fifteen micrometers, and the smallest grains were smaller than five hundred nanometers. There was variation in the grain size distribution, with certain samples exhibiting a greater range of grain sizes than others. The morphology of the grains varied as well, with some samples showing more asymmetrical geometries than others, according to the SEM imaging.

The sample became increasingly sharper and disorganized with decreasing Mn content; the FeNiCo sample exhibited the highest degree of disorder and sharpest features. Rounder and more clustered grains were observed in samples with higher Mn content. Additionally, the quantity of particles larger than three micrometers increased with the amount of Mn present. Overall, this shows how adding manganese affects the morphology and structure of the HEA and is consistent with the effects that manganese is known to have on alloys.

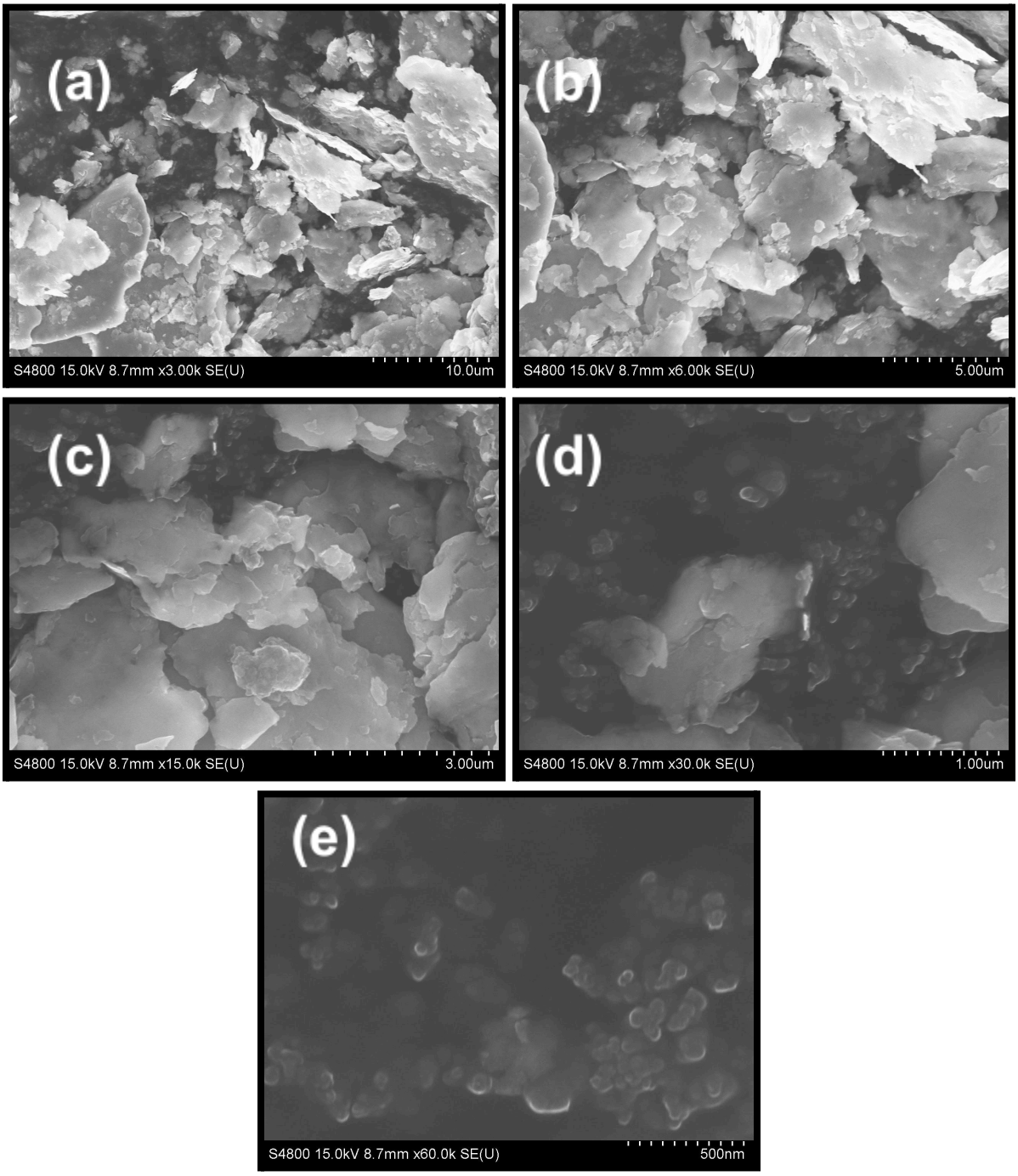

Fig. 17 SEM imaging of FeNiCo [a - e] from 10µm to 500nm

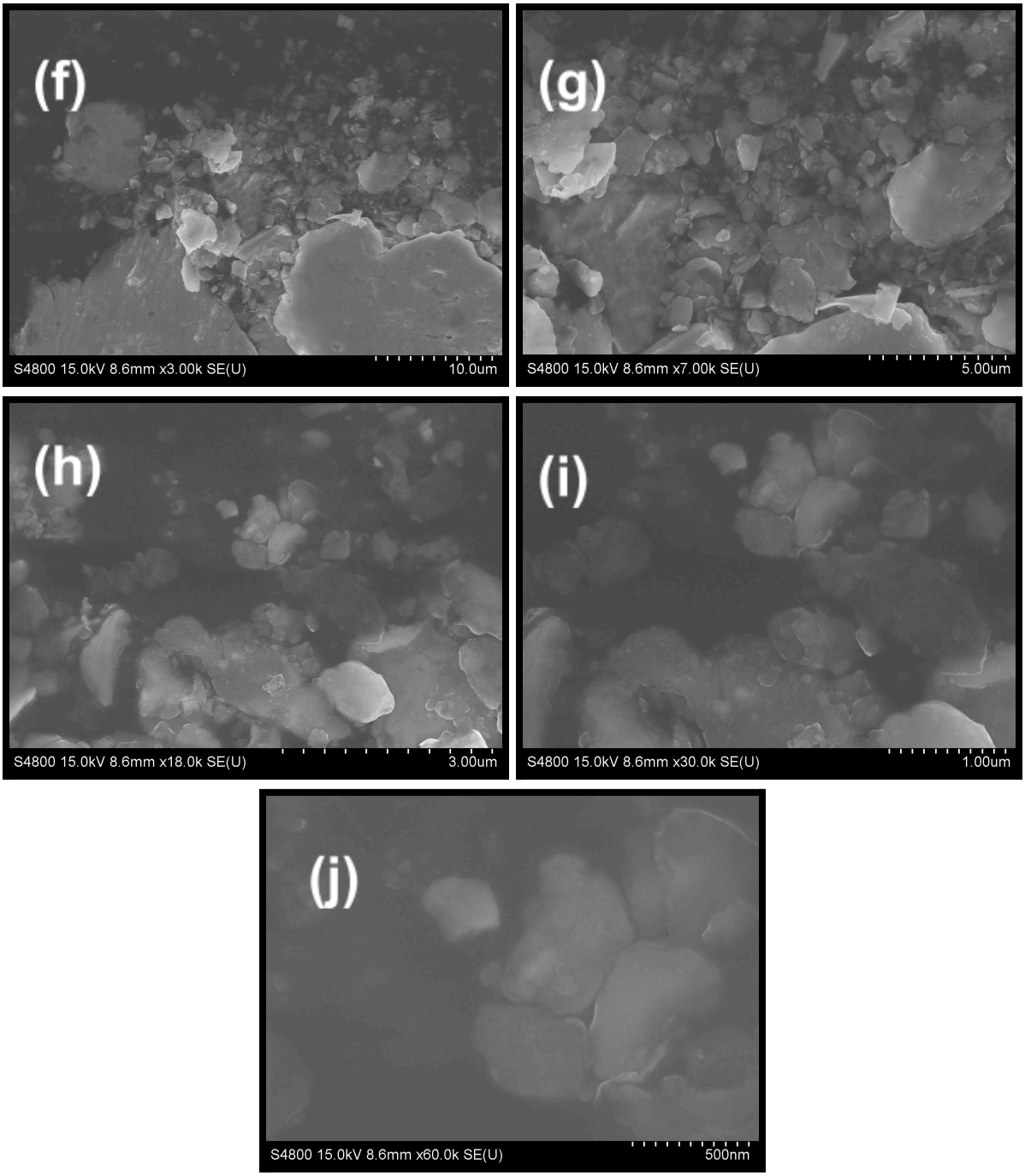

Fig. 18 SEM imaging of FeNiCo($Mn_{0.2}$) [f - j] from 10µm to 500nm

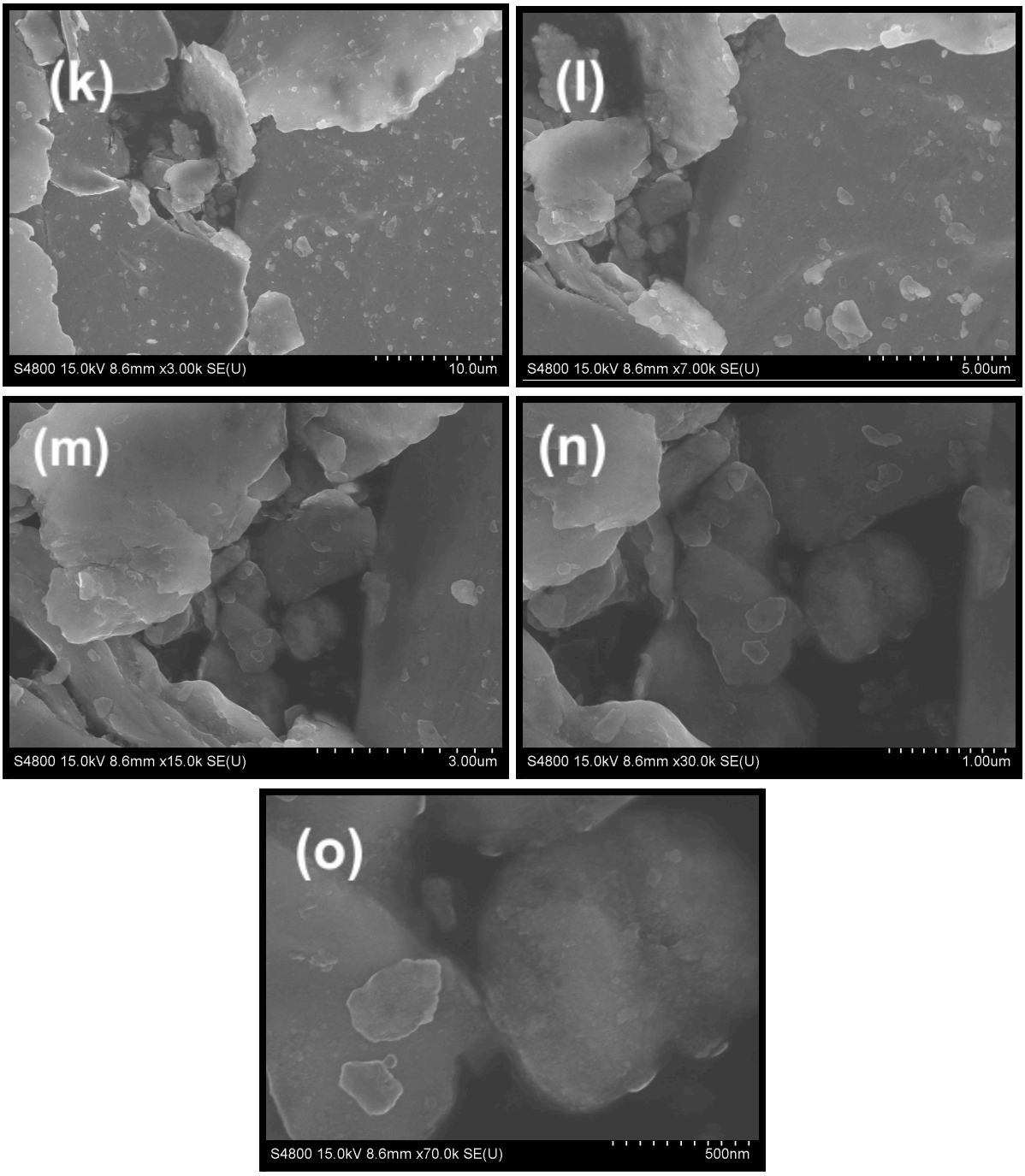

Fig. 19 SEM imaging of FeNiCo($Mn_{0.4}$) [k - o] from 10µm to 500nm

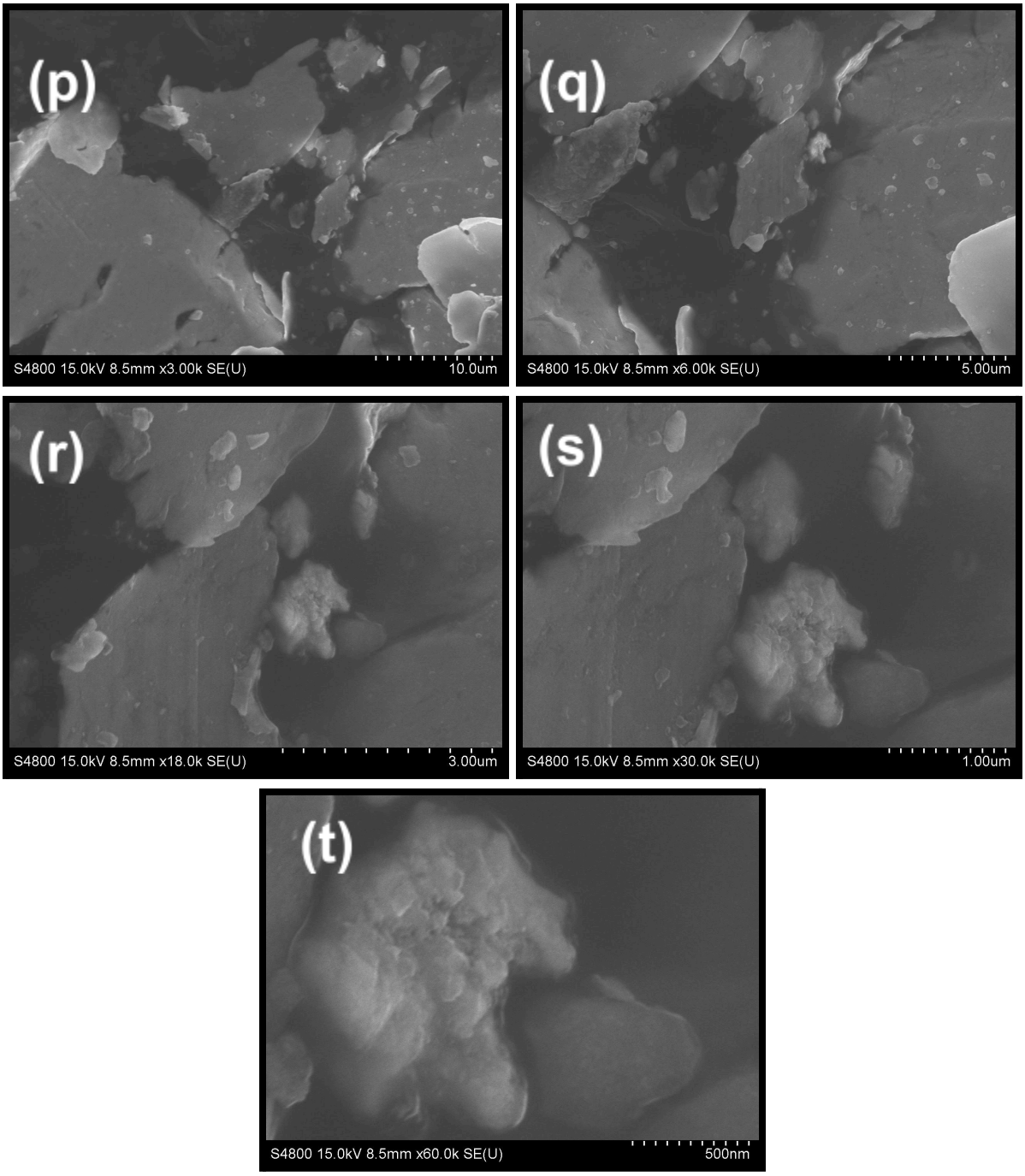

Fig. 20 SEM imaging of FeNiCo($Mn_{0.6}$) [p - t] from 10µm to 500nm

Similar to the manganese samples, SEM imaging was obtained for the $FeNiCo(Mn_{0.2}Ga_{0.1})$, $FeNiCo(Mn_{0.2}Ga_{0.3})$, and $FeNiCo(Ga_{0.2})$ samples from ~ten micrometers down to five hundred nanometers. The two samples containing manganese had more rounded features in their particles, similar to the non-gallium manganese samples. The gallium sample lacking manganese had sharper, more jagged particles. The distribution of grain sizes greater than three micrometers is increased in the presence of Mn, and the sample lacking Mn tended to have grain sizes between ten and five micrometers.

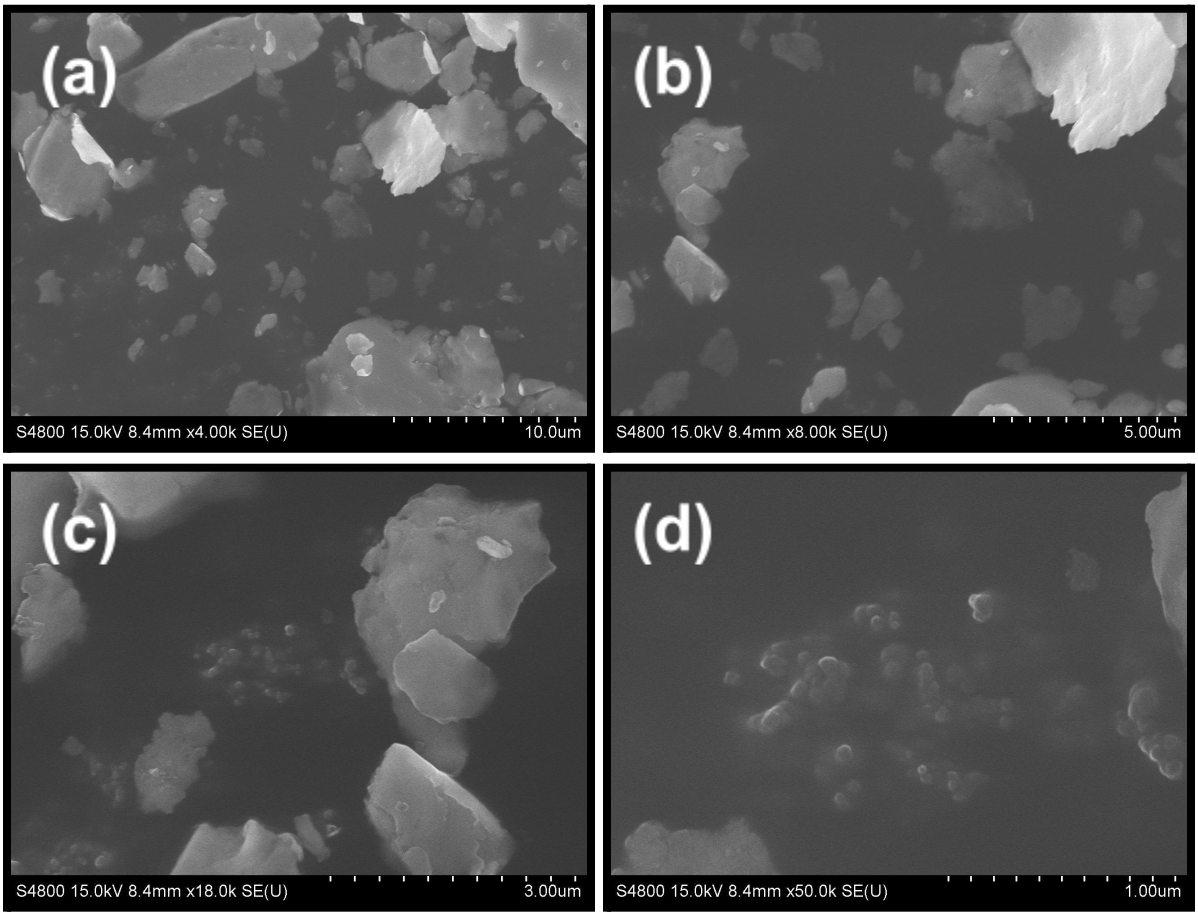

Fig 21: SEM imaging of $FeNiCo(Mn_{0.2}Ga_{0.1})$ [a - d] from 10µm to 500nm

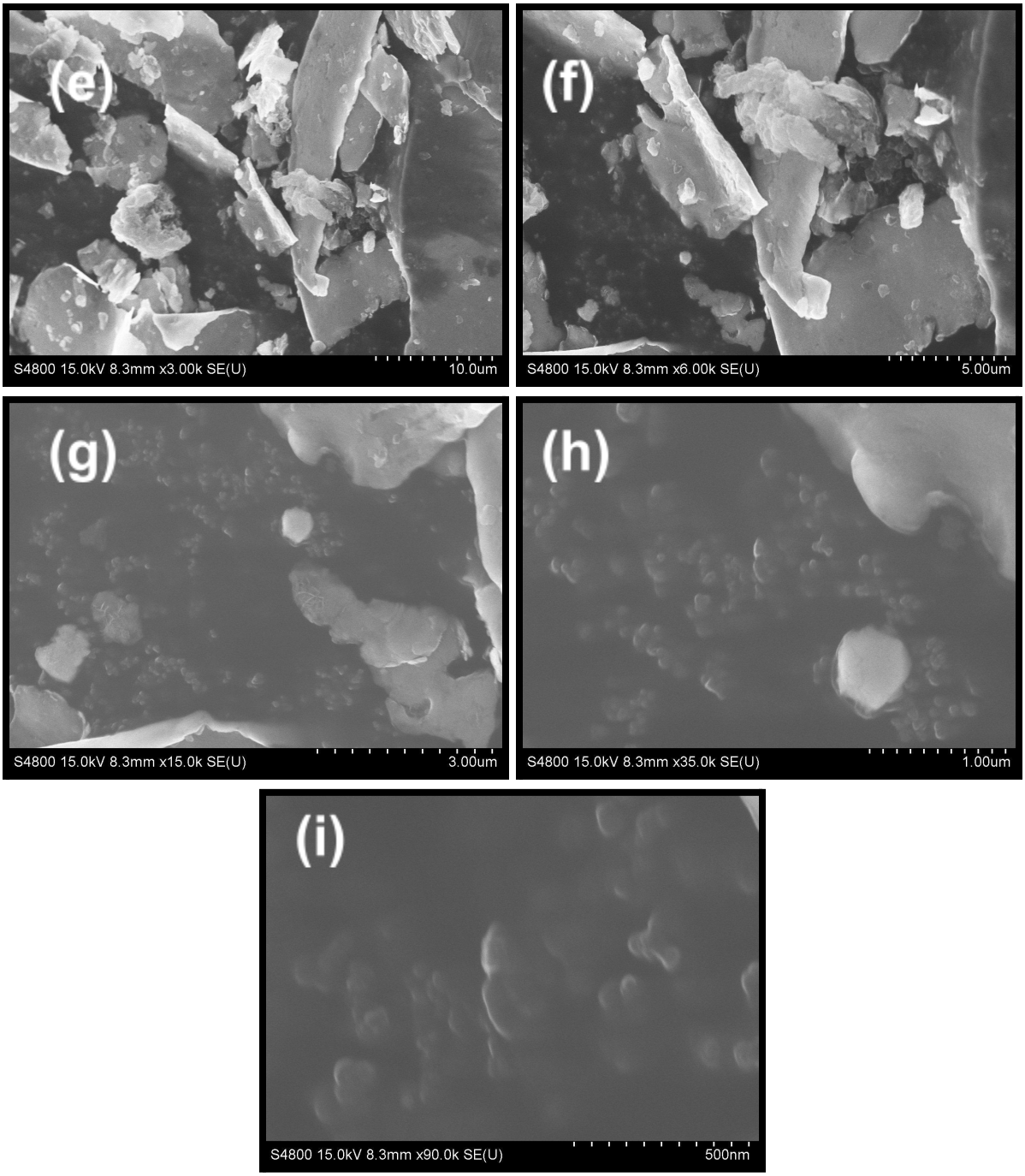

Fig 22 SEM imaging of $FeNiCo(Mn_{0.2}Ga_{0.3})$ [e - i] from 10µm to 500nm

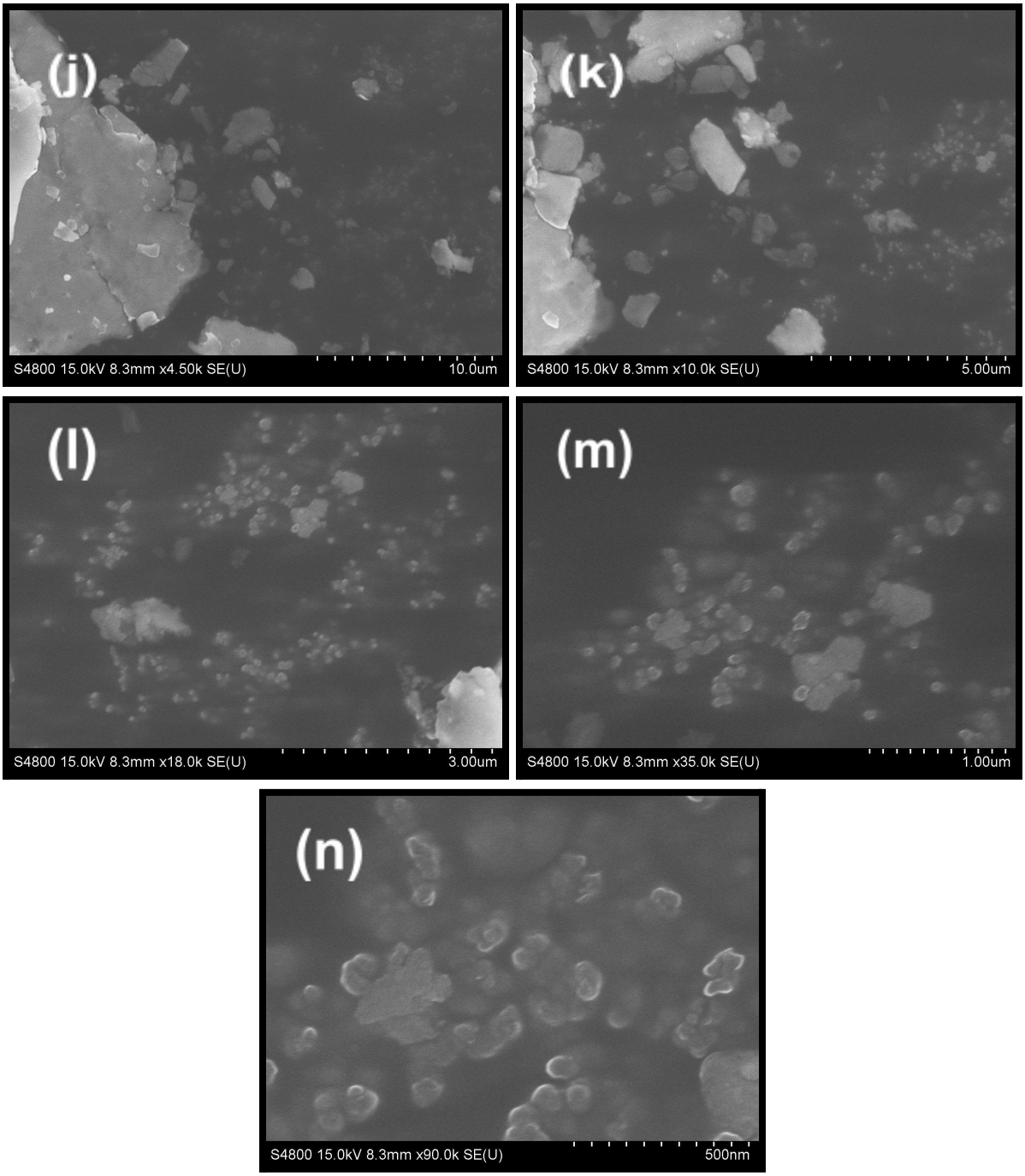

Fig 23: SEM imaging of $FeNiCo(Ga_{0.2})$ [j - n] from 10µm to 500nm

4.3 Structure and Morphology of Chemically Doped Variants

Chemically doped variations were developed to further test and evaluate the magnetic properties, structure, and morphology in comparison to the original HEA samples. Chemically doped versions of iron (Fe), nickel (Ni), and cobalt (Co) were developed to achieve this. This was accomplished by starting a chemical reaction that produced pure Fe, Ni, or Co nanoparticles, then adding $FeNiCoMn_{0.2}$ or $FeNiCoMn_{0.2}Ga_{0.1}$ powder while the mixture was still reacting. The following information was obtained by running XRD, VSM, SEM, and EDS investigations on each of the six novel HEA variations.

4.3.1 VSM Analysis

Data was gathered at both 300K and 50K when the chemically doped samples were passed through a VSM. The chemically doped variations showed slightly poorer magnetic characteristics than the previous HEA samples when the results were compared. The nickel chemically doped version of $FeNiCoMn_{0.2}$ demonstrated the highest magnetic saturation. All other samples had values that were either at or below the high Mn content samples; the lowest sample peaked at about 85.16 at 50K or 78.44 at 300K. The VSM graphs are as follows:

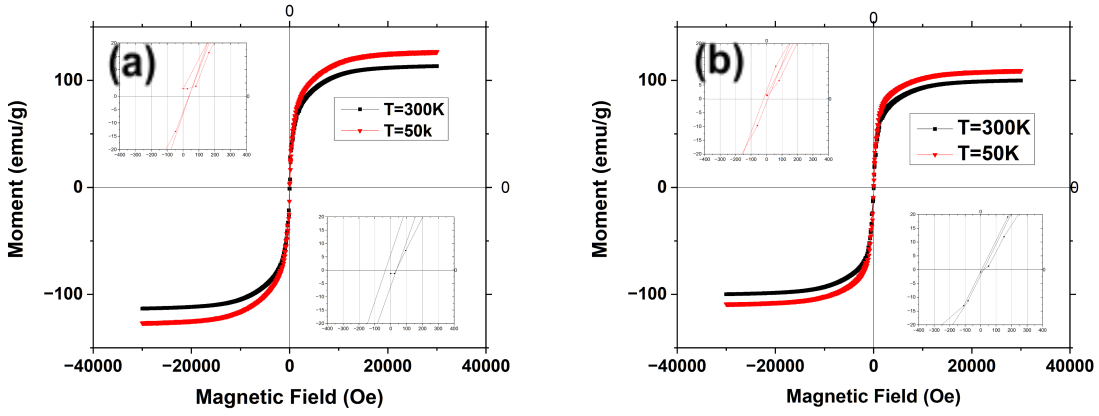

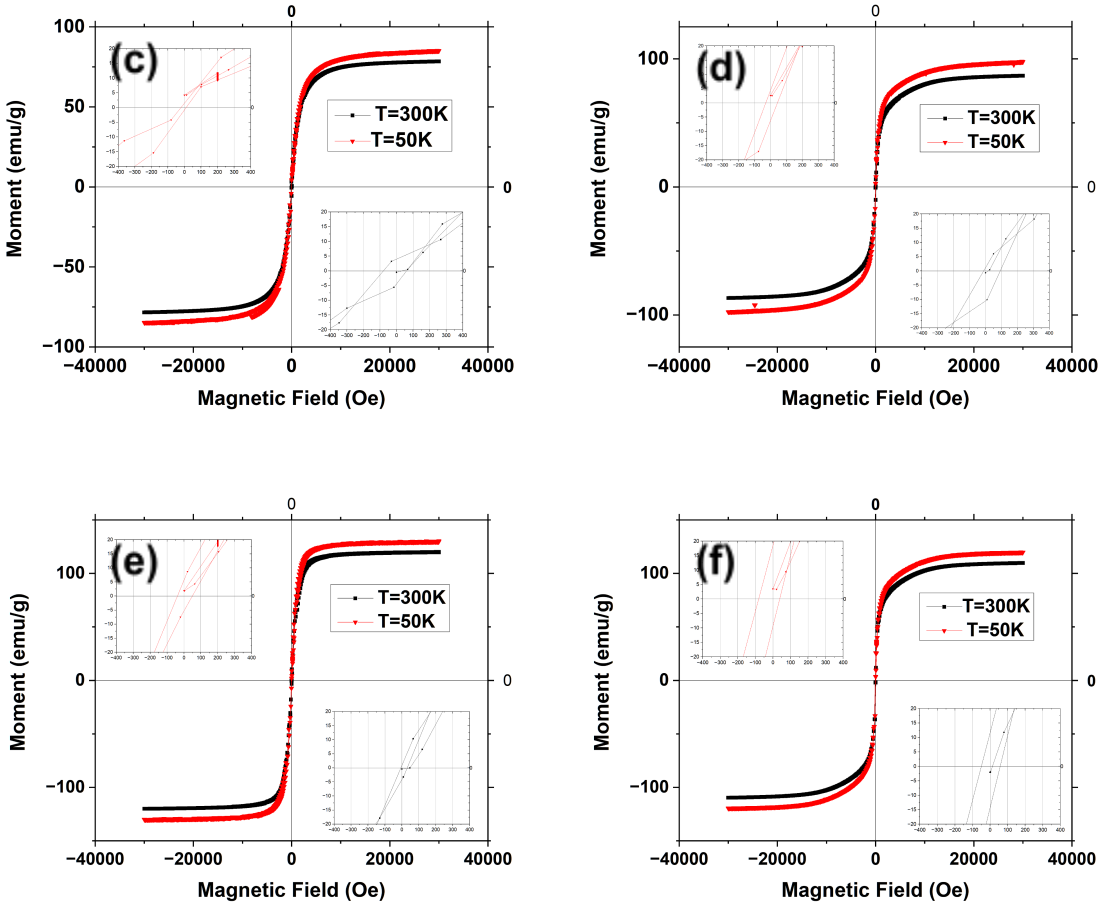

Fig. 24 Magnetic hysteresis loops of HEAs a) $FeNiCoMn_{0.2}$ Fe Doping, b) $FeNiCoMn_{0.2}Ga_{0.1}$ Fe Doping, c) $FeNiCoMn_{0.2}$ Co Doping, d) $FeNiCoMn_{0.2}Ga_{0.1}$ Co Doping, e) $FeNiCoMn_{0.2}$ Ni Doping, and f) $FeNiCoMn_{0.2}Ga_{0.1}$ Ni Doping with inset representing magnified view of central region

Chemically Doped Sample	Peak Magnetic Saturation at 50K (emu/g)	Peak Magnetic Saturation at 300K (emu/g)
$FeNiCoMn_{0.2}$ (Fe)	126.94	113.35
$FeNiCoMn_{0.2}Ga_{0.1}$ (Fe)	109.19	99.98
$FeNiCoMn_{0.2}$ (Co)	85.16	78.44
$FeNiCoMn_{0.2}Ga_{0.1}$ (Co)	97.95	86.86
$FeNiCoMn_{0.2}$ (Ni)	130.41	120.09
$FeNiCoMn_{0.2}Ga_{0.1}$ (Ni)	119.90	109.79

Table 2: Magnetic Saturation Peaks of the various HEA samples at both 50K and 300K

4.3.2 XRD Analysis

The following figures display the results of the XRD study performed on the chemically doped samples. Most peaks follow the similar trends of the base manganese and gallium samples, however the intensity of the peaks, or even their presence at all, are drastically different based on the chemical doping performed. This is indicative of the successful incorporation of the selected element.

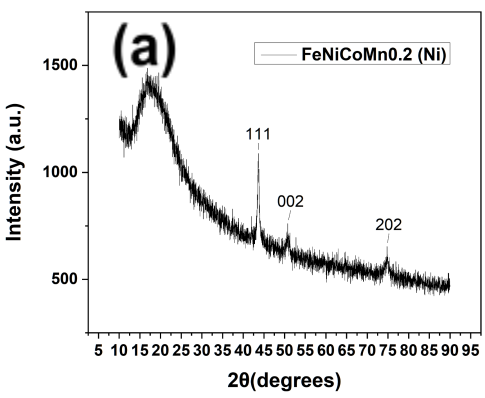

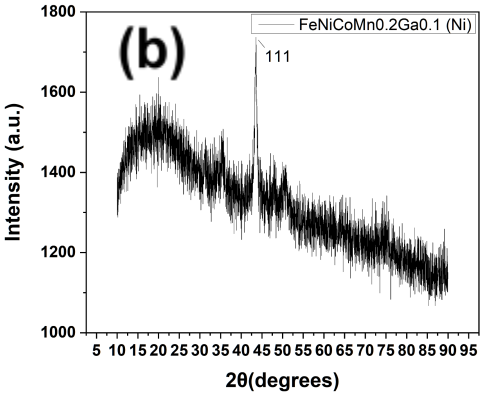

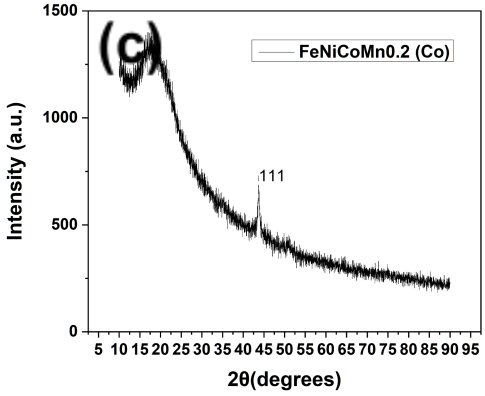

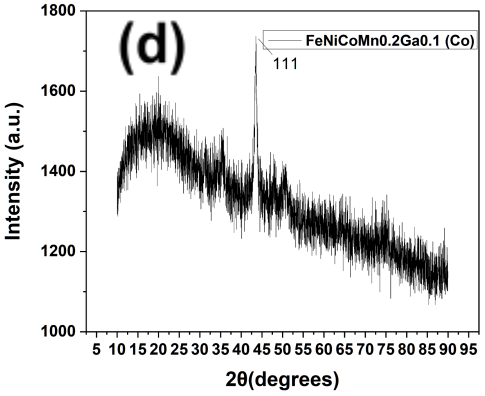

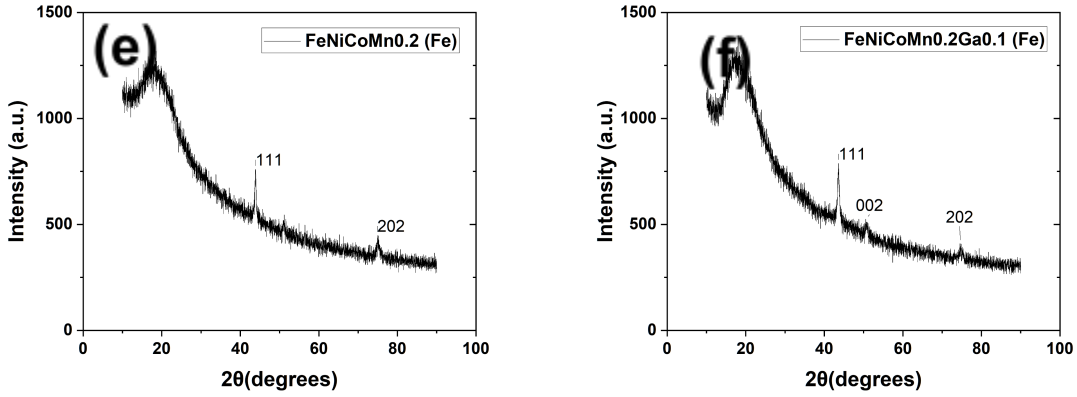

Fig. 25 XRD patterns of a) $FeNiCoMn_{0.2}$ Ni Doping, b) FeNiCoMn0.2Ga0.1 Ni Doping, c) FeNiCoMn0.2 Co Doping, d) $FeNiCoMn_{0.2}Ga_{0.1}$ Co Doping, e) $FeNiCoMn_{0.2}$ Fe Doping, f) $FeNiCoMn_{0.2}Ga_{0.1}$ Fe Doping

4.3.3 EDS Analysis

The chemically doped versions of the HEA samples show enhanced elemental presence of the selected doped element, according to the data gathered. This suggests that the surplus element was in fact integrated into the HEA, together with the changed microstructure and magnetic characteristics.

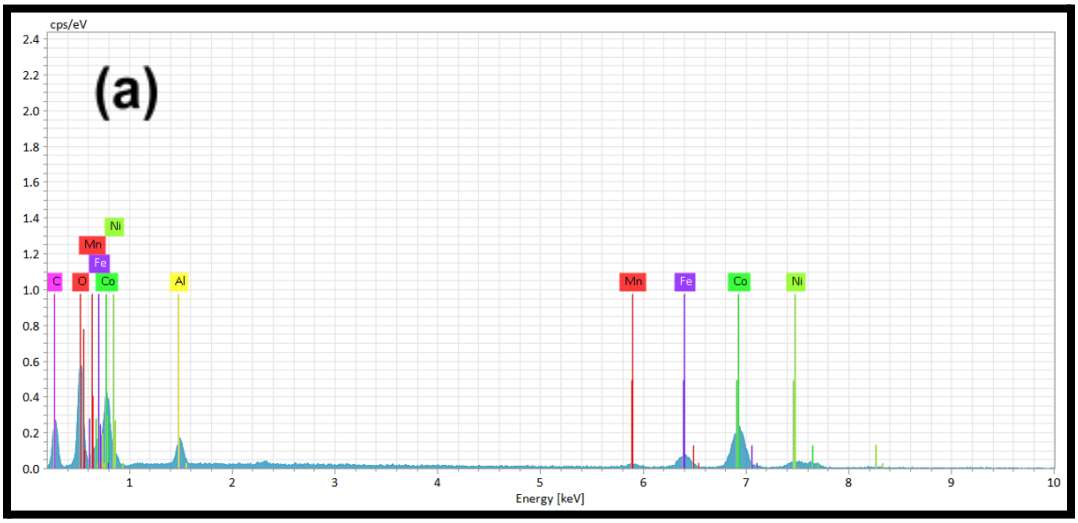

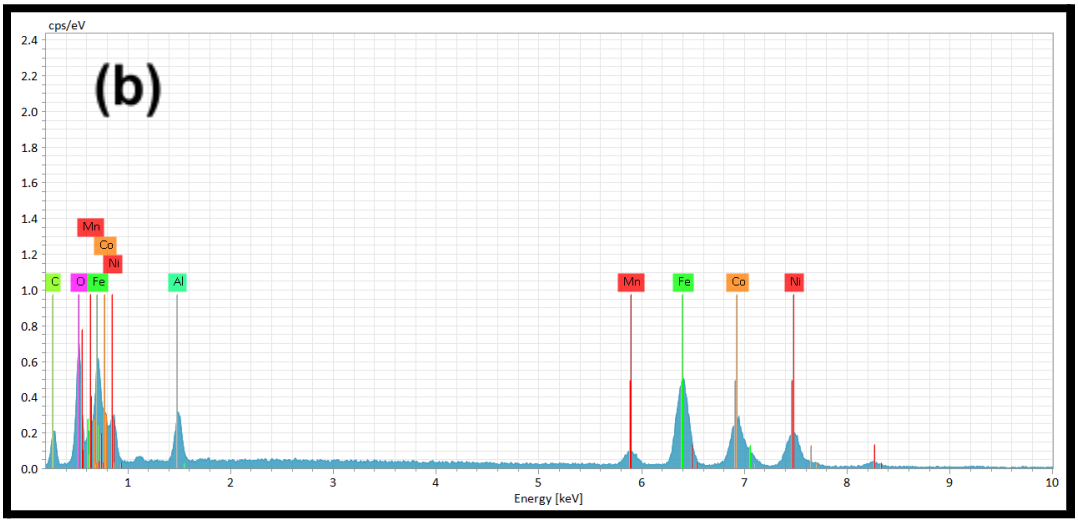

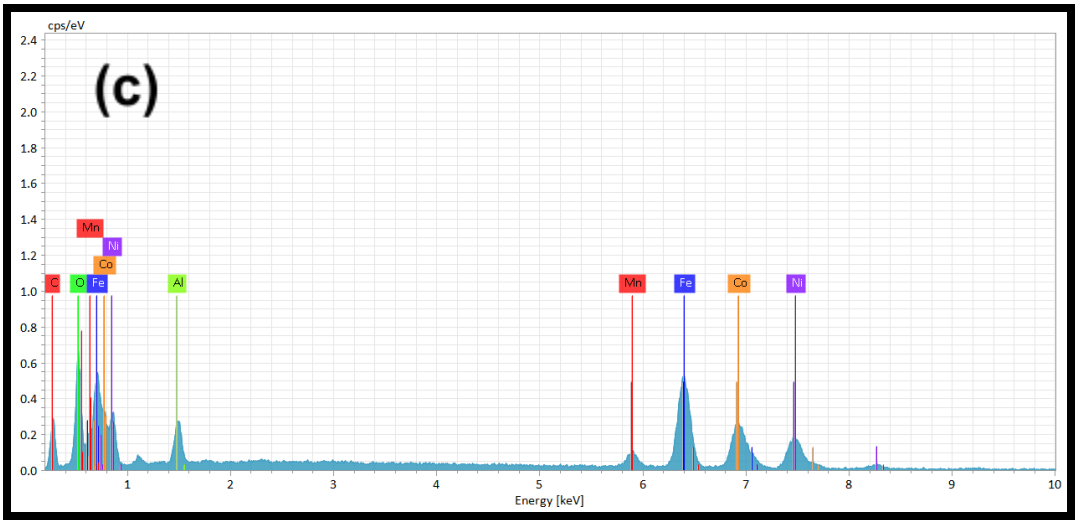
(c)
cps/eV
Energy [keV]
Mn
Ni
Co
C
O
Fe
Al
Mn
Fe
Co
Ni

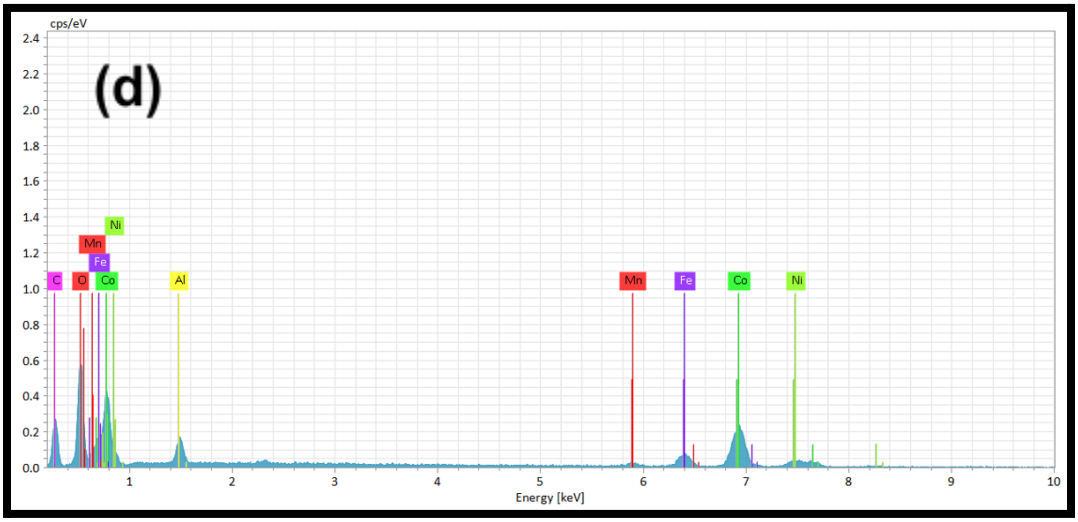
(d)
cps/eV
Energy [keV]
Ni
Mn
Fe
C
O
Co
Al
Mn
Fe
Co
Ni

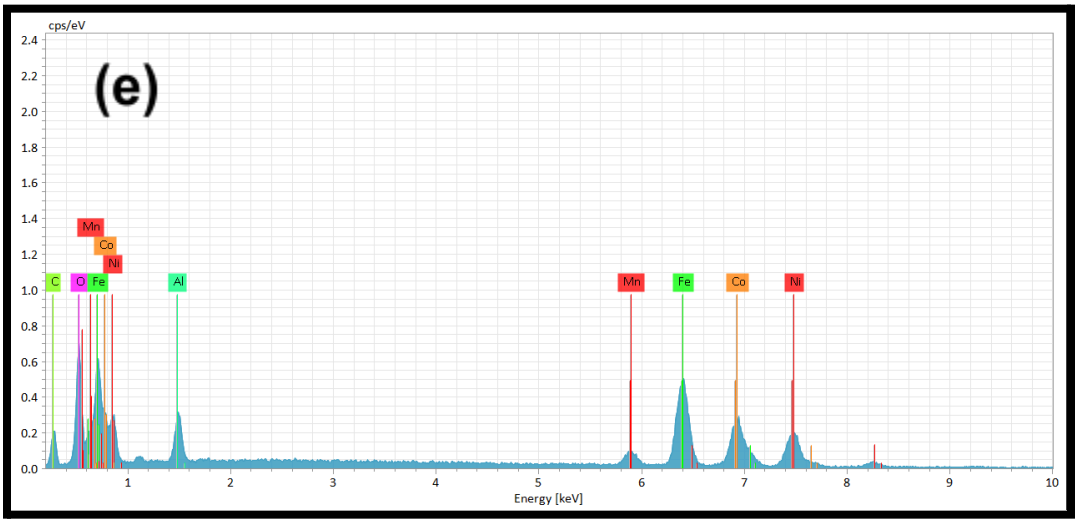
(e)
cps/eV
Energy [keV]
Mn
Co
Ni
C
O
Fe
Al
Mn
Fe
Co
Ni

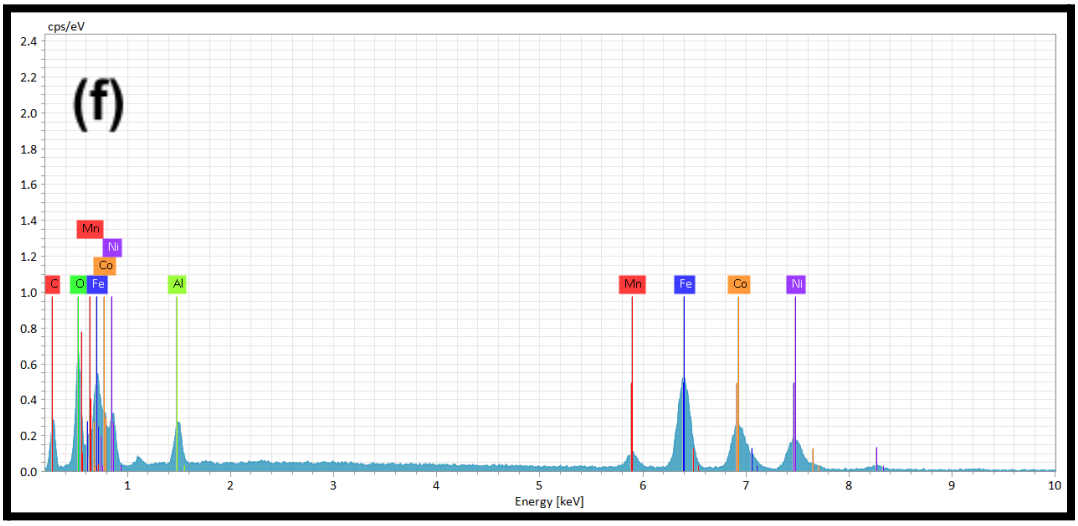

Fig. 26 EDS patterns of a) $FeNiCoMn_{0.2}Ga_{0.1}$ Co Doping, b) $FeNiCoMn_{0.2}Ga_{0.1}$ Ni Doping, and c) $FeNiCoMn_{0.2}Ga_{0.1}$ Fe Doping, d) $FeNiCoMn_{0.2}$ Co Doping, e) $FeNiCoMn_{0.2}$ Ni Doping, and f) $FeNiCoMn_{0.2}$ Fe Doping

4.3.4 SEM Analysis

To compare the microstructure of the chemically doped versions to that of the base HEA alloys, SEM imaging was conducted. Smaller, rounded particles were observed in addition to the usual microstructures. This is indicative of typical chemical synthesis and chemical doping HEA productive techniques. This is significantly more present in the cobalt and iron chemical doped variants. The cobalt doped versions exhibit significantly more grouped, spherical grains that are smaller than five micrometers.

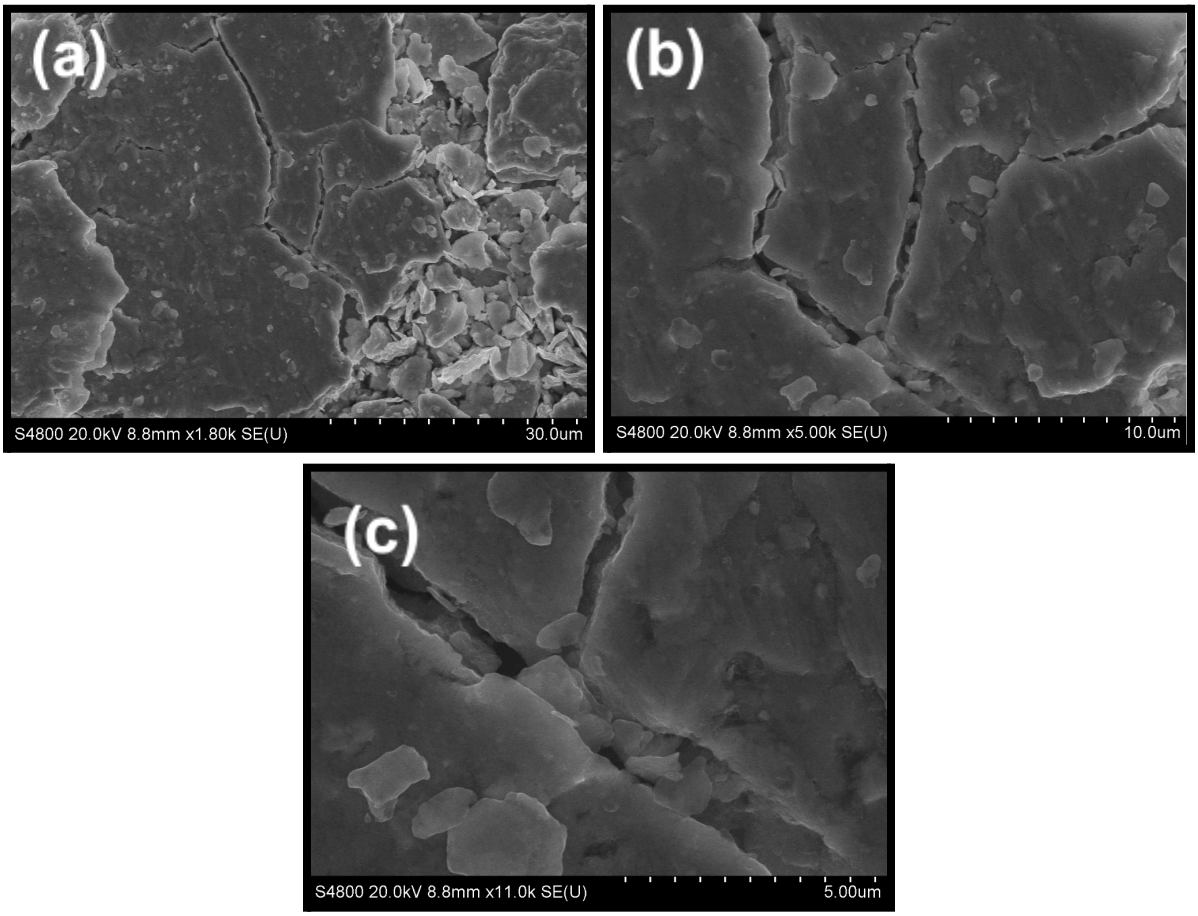

Fig. 27 SEM imaging of FeNiCoMn0.2 Ni Doping [a-c] from 30µm to 5µm

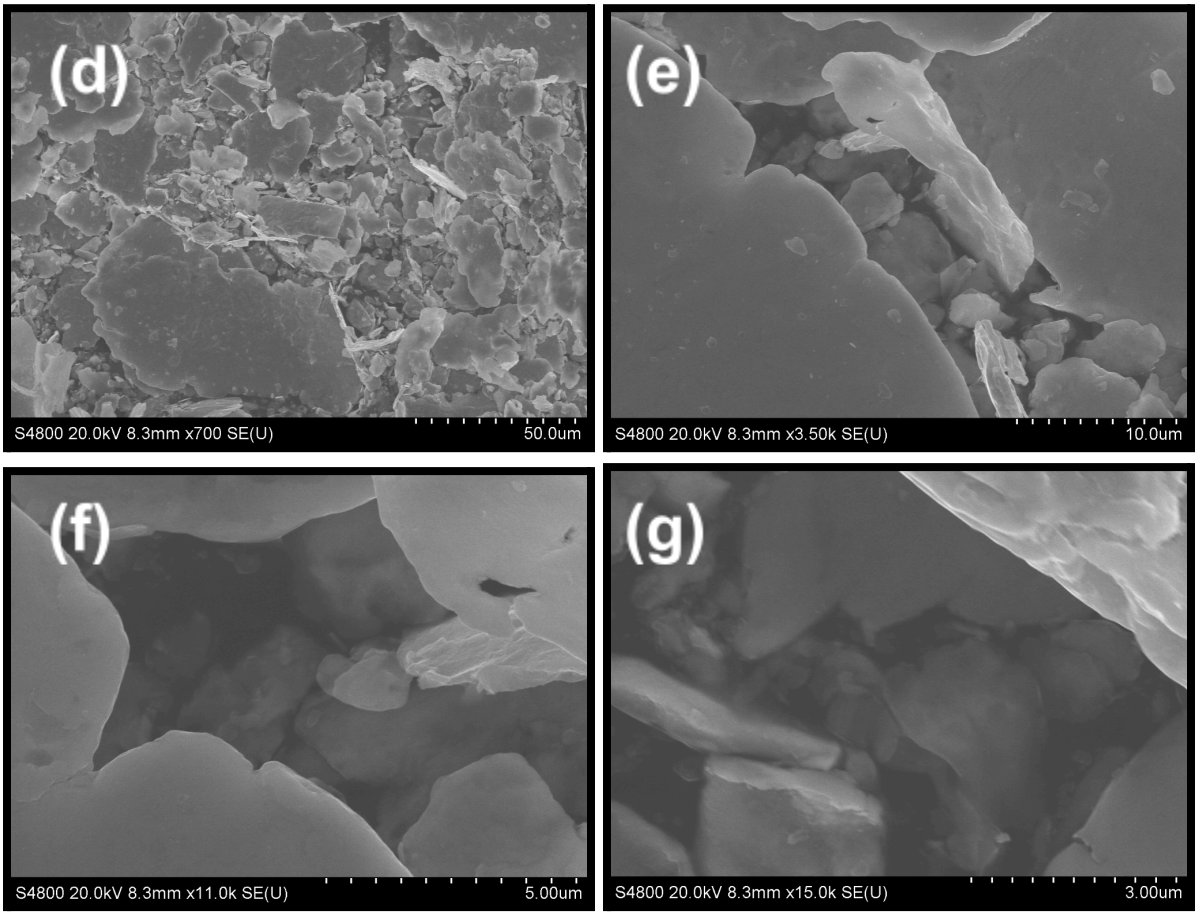

Fig. 28 SEM imaging of FeNiCoMn0.2Ga0.1 Ni Doping [d-g] from 50µm to 3µm

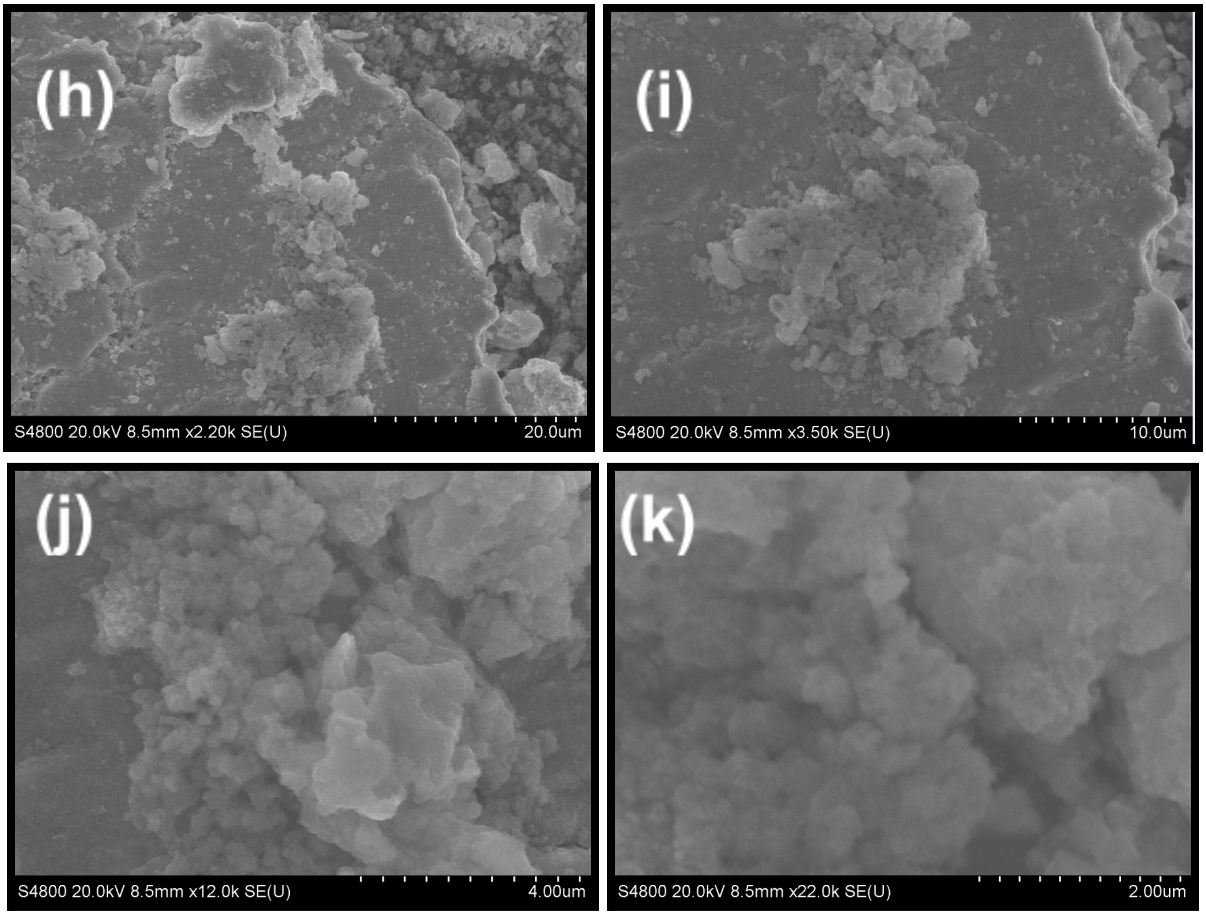

Fig. 29 SEM of imaging of FeNiCoMn0.2 Co Doping [h-k] from 20µm to 2µm

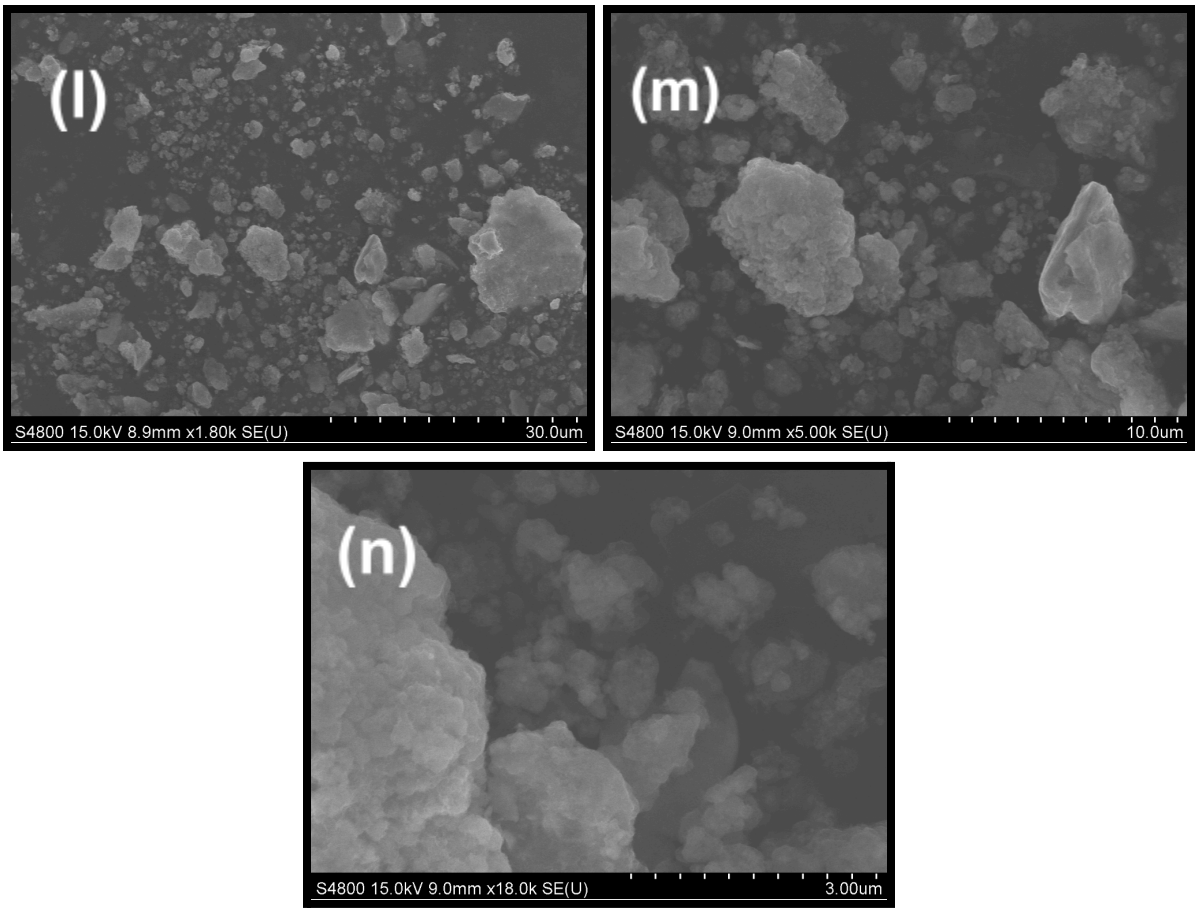

Fig. 30 SEM of imaging of FeNiCoMn0.2Ga0.1 Co Doping [l-m] from 30µm to 3µm

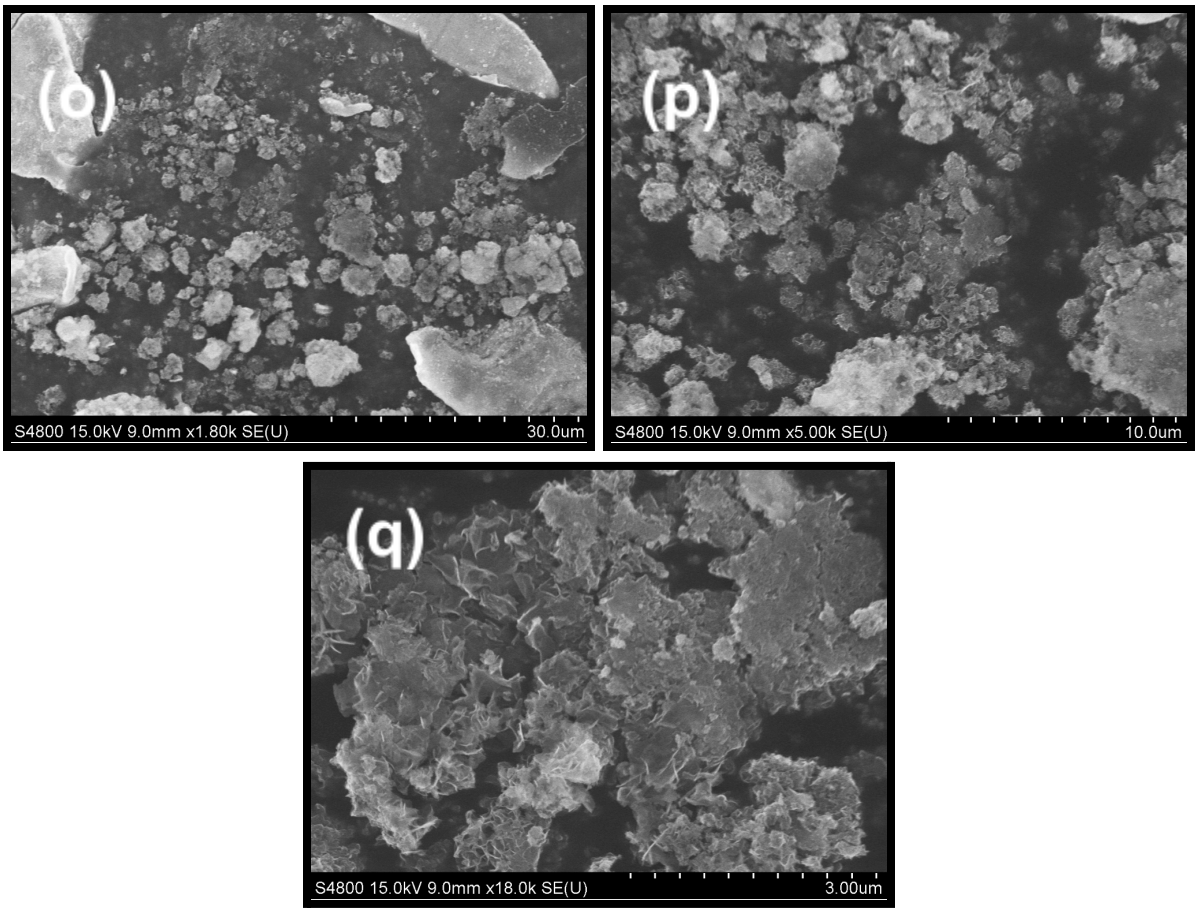

Fig. 31 SEM of imaging of FeNiCoMn0.2 Fe CS [o-q] from 30µm to 3µm

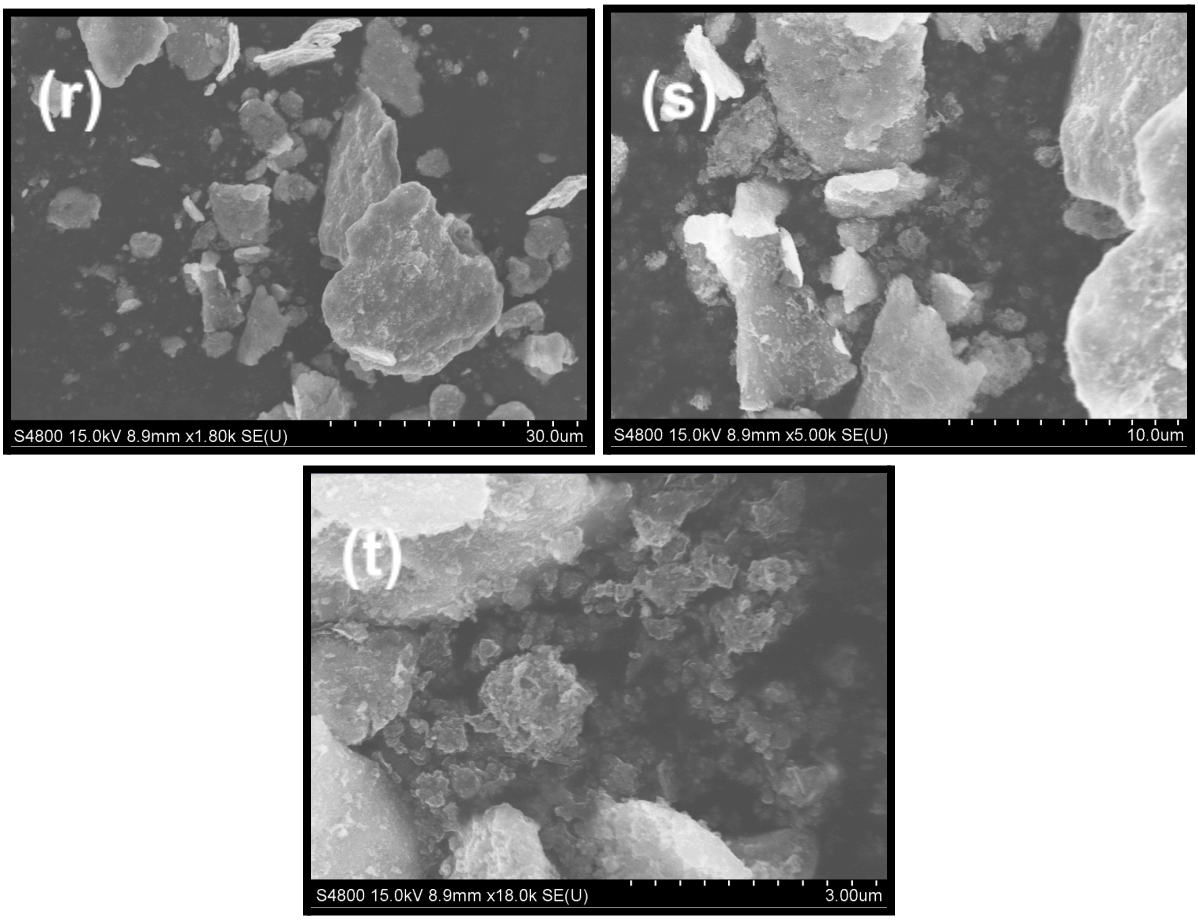

Fig. 32 SEM of imaging of FeNiCoMn0.2Ga0.1 Fe CS [o-q] from 30µm to 3µm

Chapter 5: Conclusion

The morphology, structure, and magnetic properties of the base FeNiCo HEA and its subsequent variants were thoroughly investigated. With potential use in magnetic hyperthermia, the inclusion of corrosive resistant manganese and the non-toxic gallium was incorporated into the magnetic FeNiCo. This lowered the magnetic properties of the $FeNiCoMn_{0.2}Ga_{0.1}$ and the chemical doped HEA variants in return for increased mechanical properties.

While the magnetic properties of the $FeNiCoMn_{0.2}Ga_{0.1,0.3}$ samples was lower than that of the FeNiCo, $FeNiCoMn_{0.2}$, or $FeNiCoGa_{0.2}$ samples, its structure and morphology was noticeably different. The disordered and jagged nature of the base FeNiCo HEA nanoparticles gradually became rounded, clustered grains with the inclusion of manganese and gallium. This is due in part to the mechanical benefits of both gallium and manganese introduced into the sample.

With the exception of the nickel doped $FeNiCoMn_{0.2}$, the chemically doped versions of the manganese and gallium HEA showed slightly lower magnetic characteristics. The excellent nanoparticles that the cobalt doped versions displayed was another intriguing finding.

The future of high entropy alloy (HEA) development and research looks bright, with continuous work aimed at broadening the range of compositions, enhancing processing procedures, and investigating new applications. High strength, ductility, and corrosion resistance are just a few of the special qualities that HEAs offer, and this combination of qualities makes them appealing to a variety of industries, including aerospace and energy among others. The development of new HEA materials with specialized properties for particular applications will be made possible by ongoing research into the fundamental science of HEAs and by technological advancements in synthesis and characterization.

List of Publications

Guerrero, M., Garcia, M., & El-Gendy, A. Investigation into the Magnetic Properties and Nanostructure of FeNiCoMn High Entropy Alloy. (In Progress)

References

1. Yeh, J.-W., Chen, S.-K., Lin, S.-J., Gan, J.-Y., Chin, T.-S., Shun, T.-T., Tsau, C.-H. and Chang, S.-Y. (2004), *Nanostructured High-Entropy Alloys with Multiple Principal Elements: Novel Alloy Design Concepts and Outcomes*. Adv. Eng. Mater., 6: 299-303. https://doi.org/10.1002/adem.200300567
2. Wang, Xin, Guo, Wei, Fu, Yongzhu, *High-entropy alloys: emerging materials for advanced functional applications*, Journal of Materials Chemistry A, 2050-7488, https://doi.org/10.1039/D0TA09601F
3. B. Cantor, *Multicomponent high-entropy Cantor alloys*, Progress in Materials Science, 0079-6425, https://doi.org/10.1016/j.pmatsci.2020.100754
4. George, E.P., Raabe, D. & Ritchie, R.O. *High-entropy alloys*. Nat Rev Mater 4, 515–534 (2019). https://doi.org/10.1038/s41578-019-0121-4
5. Pickering, E. J., & Jones, N. G. (2016). *High-entropy alloys: a critical assessment of their founding principles and future prospects. International Materials Reviews*, *61*(3), 183–202. https://doi.org/10.1080/09506608.2016.1180020
6. Varun Chaudhary, Richa Chaudhary, Rajarshi Banerjee, R.V. Ramanujan, *Accelerated and conventional development of magnetic high entropy alloys*, Materials Today, 1369-7021, https://doi.org/10.1016/j.mattod.2021.03.018
7. Oldřich Schneeweiss, Martin Friák, Marie Dudová, David Holec, Mojmír Šob, Dominik Kriegner, Václav Holý, Přemysl Beran, Easo P. George, Jörg Neugebauer, and Antonín Dlouhý, *Magnetic properties of the CrMnFeCoNi high-entropy alloy*, Phys. Rev. B 96, 014437, https://link.aps.org/doi/10.1103/PhysRevB.96.014437

8. Priyanka Kumari, Amit K. Gupta, Rajesh K. Mishra, M.S. Ahmad, Rohit R. Shahi, *A Comprehensive Review: Recent Progress on Magnetic High Entropy Alloys and Oxides*, Journal of Magnetism and Magnetic Materials, 0304-8853, https://doi.org/10.1016/j.jmmm.2022.169142
9. Varun Chaudhary, Richa Chaudhary, Rajarshi Banerjee, R.V. Ramanujan, A*ccelerated and conventional development of magnetic high entropy alloys,* Materials Today, 1369-7021, https://doi.org/10.1016/j.mattod.2021.03.018
10. Yih-Farn Kao, Swe-Kai Chen, Ting-Jie Chen, Po-Chou Chu, Jien-Wei Yeh, Su-Jien Lin, *Electrical, Magnetic, and Hall properties of AlxCoCrFeNi high-entropy alloys*, Journal of Alloys and Compounds, 0925-8388, https://doi.org/10.1016/j.jallcom.2010.10.210
11. Zhihua Dong, Shuo Huang, Valter Ström, Guocai Chai, Lajos Károly Varga, Olle Eriksson, Levente Vitos, *MnxCr0.3Fe0.5Co0.2Ni0.5Al0.3 high entropy alloys for magnetocaloric refrigeration near room temperature*, Journal of Materials Science & Technology, 1005-0302, https://doi.org/10.1016/j.jmst.2020.10.071
12. Pavithra, C.L.P., Janardhana, R.K.S.K., Reddy, K.M. *et al.* An advancement in the synthesis of unique soft magnetic CoCuFeNiZn high entropy alloy thin films. *Sci Rep* 11, 8836 (2021). https://doi.org/10.1038/s41598-021-87786-8
13. *FeCoNiCr0.4CuX High-Entropy Alloys with Strong Intergranular Magnetic Coupling for Stable Megahertz Electromagnetic Absorption in a Wide Temperature Spectrum*, Xiaoji Liu, Yuping Duan, Zerui Li, Huifang Pang, Lingxi Huang, Xuan Yang, Yupeng Shi, Tongmin Wang, and Xingjun Lv, Applied Materials & Interfaces 2022 14 (5), 7012-7021, https://doi.org/10.1021/acsami.1c22670

14. F. Alijani, M. Reihanian, Kh. Gheisari, *Study on phase formation in magnetic FeCoNiMnV high entropy alloy produced by mechanical alloying*, Journal of Alloys and Compounds, 0925-8388, https://doi.org/10.1016/j.jallcom.2018.09.204

15. Rajesh K. Mishra, Priyanka Kumari, Amit K. Gupta, Rohit R. Shahi, ***Design and development of Co35Cr5Fe20−xNi20+xTi20 High Entropy Alloy with excellent magnetic softness***, Journal of Alloys and Compounds, 0925-8388, https://doi.org/10.1016/j.jallcom.2021.161773

16. Zhong Li, Yong Gu, Chenxu Wang, Minxiang Pan, Huawei Zhang, Zhongyuan Wu, Xueling Hou, Xiaohua Tan, Hui Xu, *Microstructure and magnetic properties of the FeCoNi(CuAl)0.8Ga0.06 high-entropy alloy during the phase transition*, Journal of Alloys and Compounds, 0925-8388, https://doi.org/10.1016/j.jallcom.2018.11.235

17. Cheng Zhang, Qin Yu, Yuanbo T. Tang, Mingjie Xu, Haoren Wang, Chaoyi Zhu, Jon Ell, Shiteng Zhao, Benjamin E. MacDonald, Penghui Cao, Julie M. Schoenung, Kenneth S. Vecchio, Roger C. Reed, Robert O. Ritchie, Enrique J. Lavernia, *Strong and ductile FeNiCoAl-based high-entropy alloys for cryogenic to elevated temperature multifunctional applications*, Acta Materialia, 1359-6454, https://doi.org/10.1016/j.actamat.2022.118449

18. Yanchuan Tang, Neng Wan, Mingxue Shen, Haitao Jiao, Dejia Liu, Xingchang Tang, Longzhi Zhao, *A comparison of the microstructures and hardness values of non-equiatomic (FeNiCo)-(AlCrSiTi) high entropy alloys having thermal histories related to laser direct metal deposition or vacuum remelting*, Journal of Materials Research and Technology, 2238-7854, https://doi.org/10.1016/j.jmrt.2021.08.046

19. P. Thirathipviwat, G. Song, J. Jayaraj, J. Bednarcik, H. Wendrock, T. Gemming, J. Freudenberger, K. Nielsch, J. Han, *A comparison study of dislocation density, recrystallization and grain growth among nickel, FeNiCo ternary alloy and FeNiCoCrMn high entropy alloy*, Journal of Alloys and Compounds, 0925-8388, https://doi.org/10.1016/j.jallcom.2019.03.052
20. Cao, G., Liang, J., Guo, Z. *et al.* Liquid metal for high-entropy alloy nanoparticles synthesis. *Nature* 619, 73–77 (2023). https://doi.org/10.1038/s41586-023-06082-9
21. Tingting Zuo, Michael C. Gao, Lizhi Ouyang, Xiao Yang, Yongqiang Cheng, Rui Feng, Shuying Chen, Peter K. Liaw, Jeffrey A. Hawk, Yong Zhang, *Tailoring magnetic behavior of CoFeMnNiX (X = Al, Cr, Ga, and Sn) high entropy alloys by metal doping*, Acta Materialia, 1359-6454, https://doi.org/10.1016/j.actamat.2017.03.013
22. Aichi Yamashita, Tatsuma D. Matsuda, Yoshikazu Mizuguchi, *Synthesis of new high-entropy alloy-type Nb3 (Al, Sn, Ge, Ga, Si) superconductors*, Journal of Alloys and Compounds, 0925-8388, https://doi.org/10.1016/j.jallcom.2021.159233

Curriculum Vita

Matthew Guerrero was born and raised in Edinburg, Texas. Attended and graduated from Robert Vela High School with a focus on science and competed in ComSci UIL. He later went on to attend the University of Texas Rio Grande Valley and majored in Pure and Applied Physics. As an undergrad, he was given the opportunity to work in the university's Planetarium for the STEM department for one and a half years. He graduated cum laude in the spring of 2021, going on to pursue a masters degree in physics at the University of Texas at El Paso. Working as a teaching assistant during this time, he taught various courses such as General Physics 1 & 2 and Astronomy. Also during this time he helped tutor undergraduates in physics in cooperation with the UTEP Miners Learning Center.

Towards the end of his first semester in the Master program, Matthew excitedly joined the lab of Dr. Ahmed El-Gendy, focusing on the synthesis and design of High Entropy Alloys and exploring their possible magnetic characteristics. He was able to finish one publication that is in the process of being completed under Dr. El-Gendy's supervision. Now, Matthew is considering a career in aerospace, specifically with SpaceX, NASA, or Space Force.